Fall 2023

Evaluating the Effect of Resveratrol on SIRT1 with Different Peptide Substrates

Yujin Hur
San Jose State University

EVALUATING THE EFFECT OF RESVERATROL ON SIRT1 WITH DIFFERENT PEPTIDE SUBSTRATES

A Thesis

Presented to

The Faculty of the Department of Chemistry

San José State University

In Partial Fulfillment

of the Requirements for the Degree

Master of Science

by

Yujin Hur

December 2023

The Designated Thesis Committee Approves the Thesis Titled

EVALUATING THE EFFECT OF RESVERATROL ON SIRT1 WITH DIFFERENT PEPTIDE SUBSTRATES

by

Yujin Hur

APPROVED FOR THE DEPARTMENT OF CHEMISTRY

SAN JOSÉ STATE UNIVERSITY

December 2023

Ningkun Wang, Ph.D.	Department of Chemistry
Nicholas Esker, Ph.D.	Department of Chemistry
Emma Carroll, Ph.D.	Department of Chemistry

ABSTRACT

EVALUATING THE EFFECT OF RESVERATROL ON SIRT1 WITH DIFFERENT PEPTIDE SUBSTRATES

by Yujin Hur

SIRT1 is an NAD+-dependent lysine deacetylase that is involved in many important cellular pathways. The protein has an extended N-terminal domain that seems to play a role in regulating its activity. Sirtuin Activating Compounds (STACs) are allosteric activators, such as resveratrol, that regulate the activity of SIRT1. STACs bind to the N-terminal STAC Binding Domain (SBD) in SIRT1. Past literature has found that SIRT1 activity can be increased, decreased, or remain unchanged by resveratrol depending on the identity of the peptide substrate. The goal of this study is to clarify the mechanism for substrate-specific allosteric regulation by resveratrol. The interactions between resveratrol and SIRT1 remain poorly understood from a quantitative perspective. Our lab has found that resveratrol changes the enzyme activity of SIRT1 by altering its substrate recognition for different peptide substrates. Additionally, we hypothesize that the conformational changes that SIRT1 experiences upon binding to various substrates alter the way resveratrol interacts with the SIRT1•substrate complex. In turn, resveratrol may then affect SIRT1 conformation and stability in a substrate-specific manner. To this end, this study uses fluorescence-based binding assays to quantify the KD values for the SIRT1•resveratrol binding interactions in the presence of various substrates. We are also using small angle X-ray scattering (SAXS) and differential scanning fluorimetry (DSF) to determine resveratrol's effects on SIRT1 conformation and stability.

ACKNOWLEDGEMENTS

This project would not have been possible without the support of many people. Many thanks to my advisor, Dr. Wang, who read my numerous revisions and helped make some sense of the confusion. I would like to express my deepest appreciation to all the members of my research group comprised of Adorina, Addison, Bradley, Dhairya, Jenny, Nathalie, Sabrina, Malvika, Emily Quach, Emily Leong, Calvin, Ryan, Reena, Zain, Tiffany, Selina, Praagna, Patricia, My, Ayan, and Andre. Your collective knowledge, expertise, and patience have been invaluable to my research. And finally, thanks to my parents for the sacrifices you have made for me to pursue a Master's degree.

TABLE OF CONTENTS

LIST OF TABLES

LIST OF FIGURES

LIST OF ABBREVIATIONS

ADPr - Adenosine Diphosphate Ribose
CV - Column Volume
DSF - Differential scanning fluorimetry
DTT - Dithiothreitol
ESA - Essential for Sirtuin Activity
FPLC - Fast Protein Liquid Chromatography
IPTG - Isopropyl ß-D-1-Thiogalactopyranoside
ITC - Isothermal Titration Calorimetry
LB - Luria Broth
NAD+ - Nicotinamide Adenine Dinucleotide
Ni-NTA - Nickel-Nitrilotriacetic Acid
OAADPr - O-acetyl-ADP-ribose
PCR - Polymerase Chain Reaction
SAXS - Small Angle X-ray Scattering
SBD - STAC Binding Domain
SDS -PAGE- Sodium Dodecyl Sulfate–Polyacrylamide Gel Electrophoresis
SEC - Size Exclusion Chromatography
SIRT1 - Sirtuin (Silent Mating Type Information Regulation 2 Homolog) 1
Sir2 - Silent information regulator 2
STAC - Sirtuin Activating Compound
SUMO - Small Ubiquitin Modifying Protein
WT - Wild-type

1 INTRODUCTION

1.1 Background of SIRT1

The protein known as SIRT1 belongs to the sirtuin family of enzymes, which function as physiological modulators by catalyzing a deacetylase reaction and are genetically conserved from bacteria to humans.[1] In recent years, SIRT1 has emerged as a highly desirable focus for scientific investigation due to the numerous essential roles it plays in maintaining cellular homeostasis (Figure 1.1).[2] A rise in the incidence of age-related illnesses and metabolic disturbances such as neurodegeneration, and diabetes has driven the hunt for potential treatment methods that target SIRT1 and its regulatory mechanisms.[1] In summary, SIRT1's potential therapeutic implications have contributed to its status as a very important research subject. However, study of SIRT1 remains difficult due to the lack of concrete information on its regulation, specifically the underlying mechanism and conformational structure. Additionally, the full length SIRT1 protein is unstable when expressed in vitro, denaturing readily in enzyme assays.

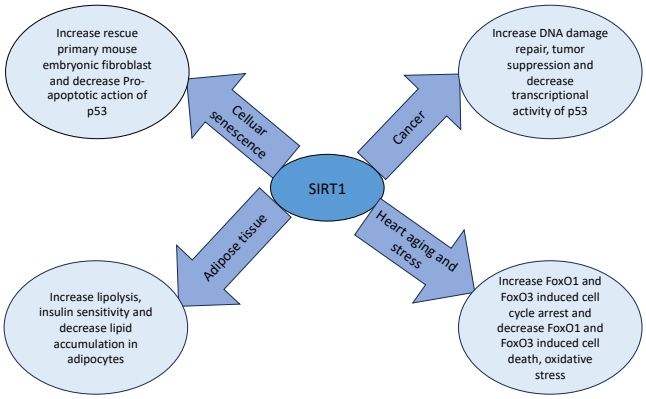

Figure 0.1. Summary of the SIRT1's main characteristics and its function in cellular regulation.[3]Sir2 (silent information regulator 2) was the first of a family of enzymes called sirtuins to be discovered. The discovery of yeast Sir2 was essential to the study of sirtuins due to their role in modulating metabolic pathways. SIRT1 is the closest homolog to Sir2 among the seven sirtuins identified in humans (SIRT1-7). Each sirtuin has a conserved 275-amino-acid catalytic core domain and variable-length N- and C-terminal regions (Figure 1.2).[1]

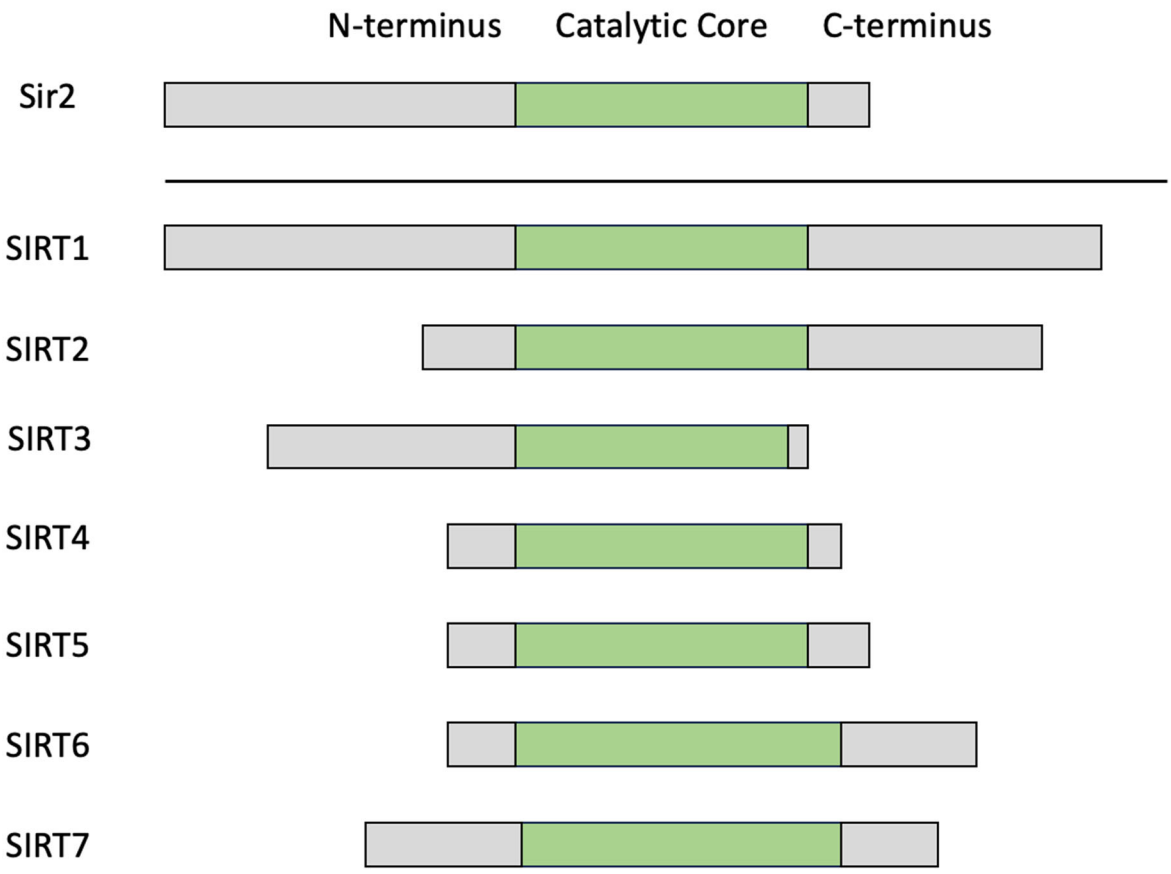
N-terminus
Catalytic Core
C-terminus
Sir2
SIRT1
SIRT2
SIRT3
SIRT4
SIRT5
SIRT6
SIRT7

Figure 0.2. A structural review of year Sir2 and mammalian Sirtuin. The green region is the catalytic core, the left gray region is the N-terminus, and the right gray region is the C-terminus. The longest N- and C-termini are on SIRT1.[1]SIRT1 is made up of 747 amino acid residues. The N-terminal region is located at the beginning of the protein sequence, followed by the catalytic core domain and the C-terminal region which is located at the end of the protein sequence. In particular, the catalytic core consists of a highly conserved Rossmann-fold domain and a minor domain with a zinc-binding module and a helical module. The interaction between the acetylated residue of the protein substrate and NAD^+ with SIRT1 through the cleft in between two domains initiates catalytic activities.[4] Both the N-terminal and the C-terminal portions of SIRT1 contribute to the protein's ability to catalyze reactions more effectively. The N-terminal domain makes a considerable contribution to the catalytic rate, and this contribution is generally unaffected by the type of the acetyl-lysine protein substrate. On the other hand, the C-terminal domain makes a significant contribution to the K_M value for NAD^+.[5] A sequence of 25 amino acids is found at the C-terminus of SIRT1, and this region is called essential for SIRT1 activity (ESA), which is located between residues 641-655. This region connects with the deacetylase core and serves as its "on switch". The ESA motif can be covalently linked to the central catalytic site of SIRT1 to stimulate its enzymatic activity and substrate binding capacity.[6] Allosteric modulators of SIRT1, or STACs (Sirtuin Activation Compounds), bind to a location on SIRT1's N-terminus termed the STAC binding domain (SBD)[7], which is connected to the catalytic domain via a flexible loop region (Figure 1.3).

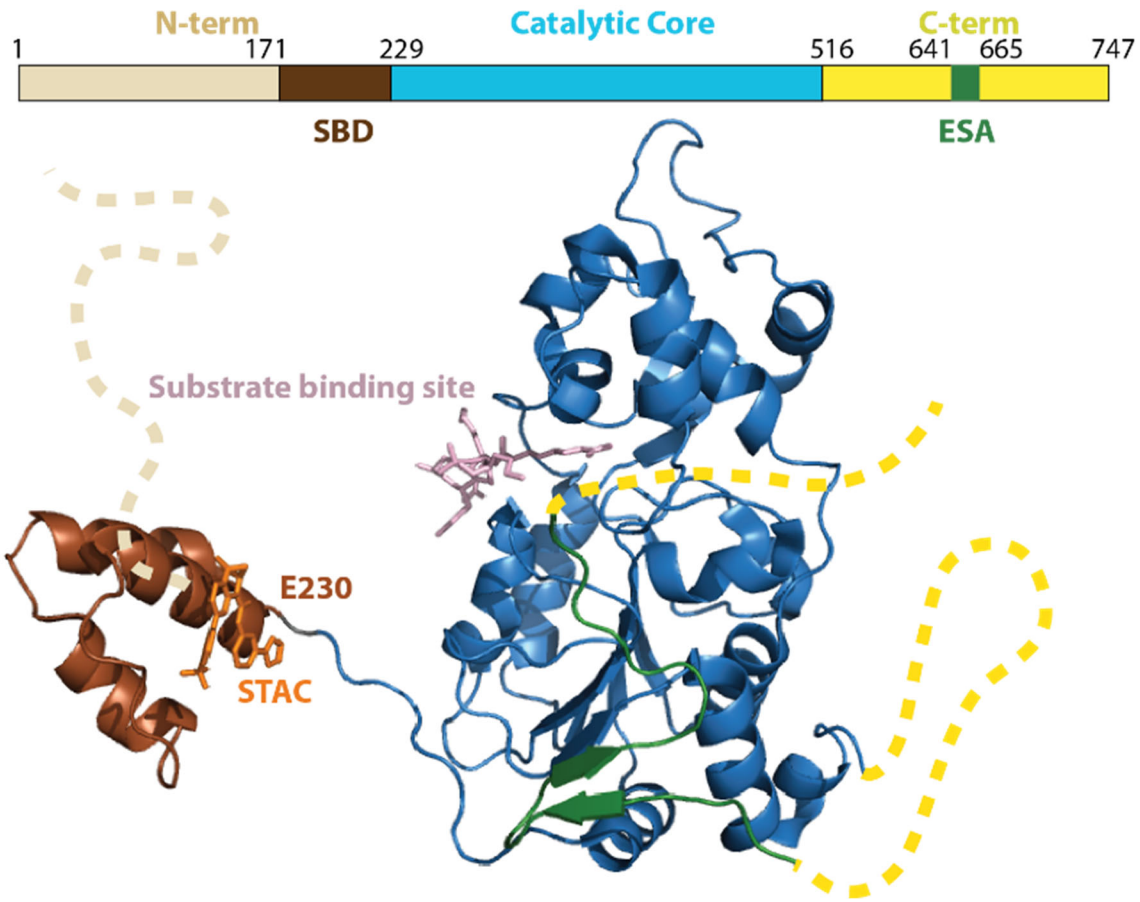

Figure 0.3. Sequence and structural summary of SIRT1 (PDB 4ZZJ) with the catalytic core shown in blue, the N-terminal's SBD is shown in brown, and C-terminal's Essential for SIRT1 Activity (ESA) domain shown in green completing the beta sheets at the Rossman fold. Unstructured N- and C-terminals shown as dashed lines.

SIRT1's deacetylase activity is dependent on the presence of its cosubstrate NAD^+. A conformational shift in SIRT1 that occurs after binding to NAD^+ permits it to hydrolyze the NAD^+ molecule. This reaction yields nicotinamide and creates O-acetyl-ADP-ribose (OAADPr). The OAADPr molecule transfers the acetyl group from a substrate protein to its 2' ribose oxygen to create deacetylated protein substrate and 2'-O-acetyl-ADP-ribose (O-Ac-ADPR) (Figure 1.4).

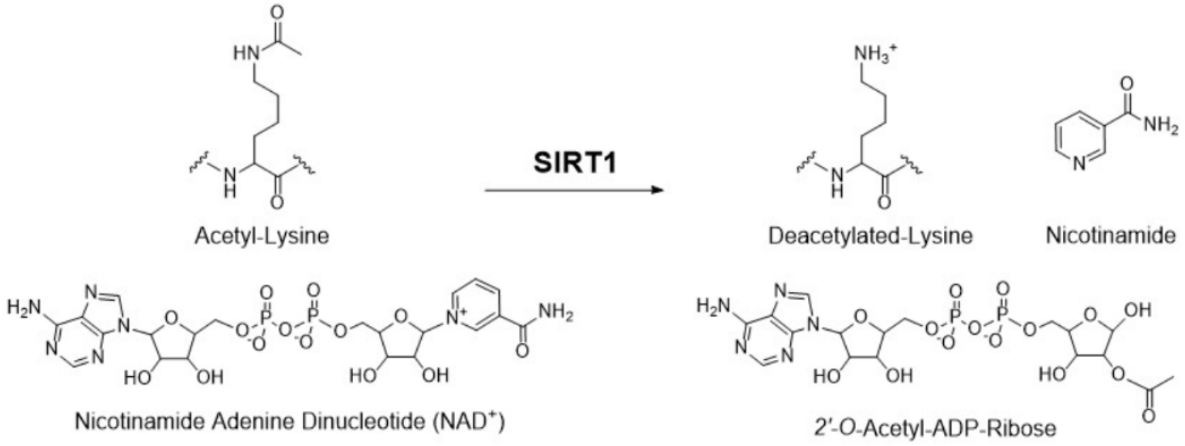

Figure 0.4. Reaction scheme illustrates how SIRT1 deacetylates lysine.[1]**1.2. Conformational Changes of SIRT1**

Previous structural studies have shown that conformational changes occur in the catalytic core of SIRT1 upon binding to NAD^+.[4] In the absence of NAD^+, SIRT1 adopts a conformation known as the "open" state. This configuration is not optimal for catalytic activity. After NAD^+ binding, the two subdomains of SIRT1 catalytic core come together and form a "closed" state (Figure 1.5). In general, the conformational changes that take place following NAD^+ binding are essential for the enzymatic activity and substrate recognition of SIRT1, and they play an important part in the regulation of metabolic activities.[4]

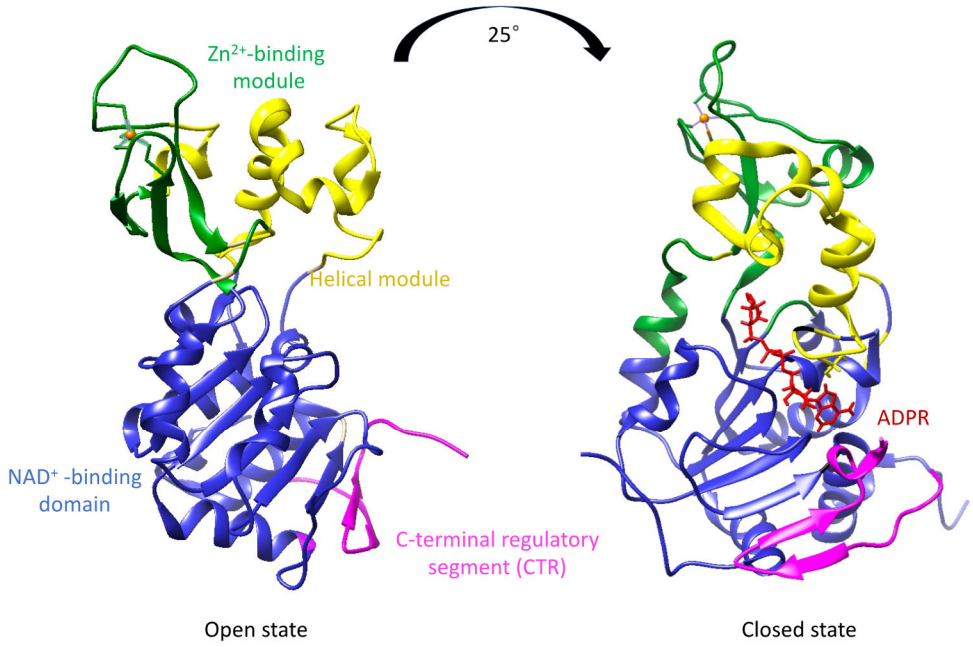

Figure 0.1.Reaction scheme of conformational changes and activation of SIRT1.[4]There is also possibly important conformational change of the STAC-binding domain (SBD) in relation to the catalytic core.[7] Previous research showed that STACs can improve substrate binding to SIRT1, resulting in an overall increase in SIRT1 catalytic efficiency.[7] The complete elimination of the SBD effectively eradicates the STAC-mediated activation of SIRT1, thereby proving the essential role of this domain in the process of activation by STACs.[7]

The analysis of previous SIRT1 structures has revealed that the loop connecting the substrate-binding domain (SBD) and the catalytic core exhibits flexibility. Additionally, the conformation of the SBD in relation to the catalytic core displays significant fluctuations. Furthermore, earlier investigations have demonstrated that the three helices comprising the SBD can become disordered and reduced bundling when interacting with inhibitor

proteins.[8,7,9] It is possible that when a small molecule SIRT1 activator is present, it induces an interaction between the SBD and the catalytic core of SIRT1, resulting in a conformational shift that triggers the activation of the enzyme (Figure 1.6). The coupling of STAC binding in the N-terminal region and substrate affinity within the catalytic region of SIRT1 suggests that allosteric regulation plays a key role; however, the role of individuals substrates remains uncharacterized. We hypothesize that various substrates would elicit distinct changes to SIRT1 conformation, thus resulting in differential interactions with resveratrol.

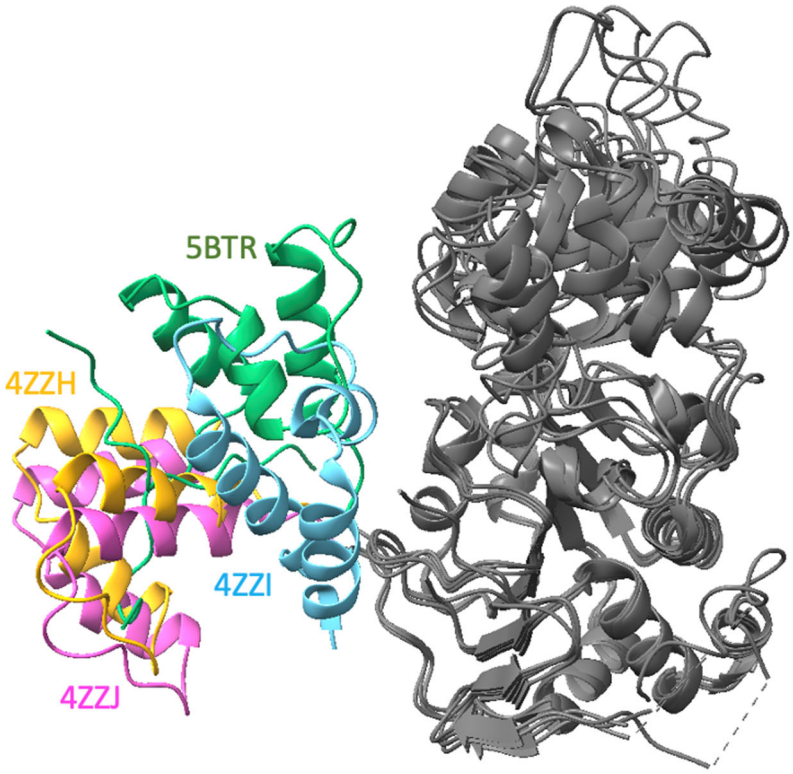

Figure 0.2. Overlays of all the SIRT1 structures that include the SBD, highlighting the different SBD positions in color and the catalytic core in gray.

1.3. Regulation of SIRT1 by Resveratrol in Previous Studies

Resveratrol is a naturally occurring molecule that can be found in red wine (Figure 1.7). It has been hypothesized that resveratrol could be responsible for the activation of SIRT1, which would then result in possible health benefits.[10] However, the mechanisms for resveratrol regulation of SIRT1 are not completely understood yet.

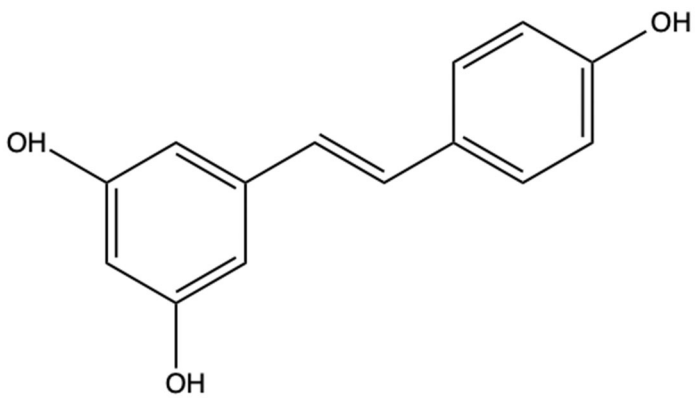

Resveratrol

Figure 0.1. The structure of resveratrol. During initial studies, the compound resveratrol was suggested to be an effective activator. It was shown that resveratrol did not have a substantial impact on the catalytic rate (k_{cat}) measurement when either the substrate (p53) or NAD^+ were altered. However, it did have a noticeable influence on the Michaelis constant (K_M) with the variable substrates.[11] Additional experiments have shown that the activating impact of resveratrol is contingent upon the utilization of the fluorescent substrate, namely p53-AMC (7-Amino-4-methylcoumarin), suggesting a potential artifact in the enzyme activity assay. As a result, the efficacy of resveratrol in augmenting SIRT1 activity against native substrates like as p53 has been a subject of debate, raising questions over its direct activation potential. Further research has shown that resveratrol has the ability to activate SIRT1 on substrates that have large hydrophobic groups. Furthermore, the analysis of a crystal structure of SIRT1 in conjunction with p53-AMC has shown the coordinated binding of three resveratrol molecules.[10]

To research the impact of SIRT1 activation induced by resveratrol on physiological deacetylation sites, previous studies utilized peptide microarrays.[12] The study including 6,802

distinct acetylated peptide substrates derived from the mammalian acetylome and showed that resveratrol has variable effects on SIRT1; indeed, it could function as either an activator or inhibitor or have no impact depending upon the specific peptide substrate sequence.[12]

In other studies focusing on the interaction between resveratrol and SIRT1, resveratrol had a stronger affinity for SIRT1 in the presence of peptide substrate.[13] The result implies that the process of SIRT1 interaction with a substrate may result in a conformational change that allows the allosteric binding site to bind to its ligand more efficiently. Furthermore, the results reveal that the mechanism of SIRT1 regulation by the activator is dependent on the substrate. The investigation suggests that the binding of resveratrol to SIRT1 facilitates substrate binding by decreasing the K_D value of SIRT1 and Ac-p53 peptide, thereby enhancing SIRT1 activity. The affinity of resveratrol towards the SIRT1-Ac-p53 peptide complex is higher, hence emphasizing the complex interaction among SIRT1, activator, and substrate.[13]

Table 0.1.
A Summary of Michaelis-Menten Kinetics Parameters of SIRT1 Activity Against Various Peptide Substrates with and without the Addition of 0.2 mM Resveratrol

Peptide Substrates	**Resveratrol**	k_{cat} **(s^{-1})**	K_M **(μM)**
Ac-p53W (STSRHKK^{Ac}WMFKTE)	-	0.06 ± 0.001	13 ± 1.4
	+	0.06 ± 0.004	6 ± 1.0
Ac-p53 (STSRHKK^{Ac}LMFKTE)	-	0.08 ± 0.009	25 ± 0.2
	+	0.07 ± 0.002	61 ± 1.6
Ac-H4 (VRGKAGK^{Ac}GLGKGG)	-	0.09 ± 0.006	108 ± 5.5
	+	0.07 ± 0.005	217 ± 23.2
Ac-H3 (KSTGGK^{Ac}APRKQ)	-	0.06 ± 0.009	121 ± 12.6
	+	0.05 ± 0.002	183 ± 8.9
Ac-CSNK (ASSSGSK^{Ac}AEFIVG)	-	0.06 ± 0.002	78 ± 2.2
	+	0.09 ± 0.036	519 16.9

1.4. Using SAXS to Study Conformational Changes in SIRT1

Small angle X-ray scattering (SAXS) has been used to examine conformational changes in multimodular proteins. Indeed, this method is an essential technique for the investigation of biological molecules in solution.[14] This technique could provide a precise and comprehensive understanding of the protein's conformational dynamics in a solution-based environment. For example, Hodge et al. used SAXS to analyze the purified complexes' structure and flexibility in the solution. In their investigations, the findings show that RING E3 RNF8 moves E2 Ubc13 to double-strand break sites and plays a key role in damage feedback by activating polyubiquitination by changing the shape of ubiquitin that is covalently linked to the Ubc13 active site.[15] The experimental scattering pattern provides direct information on several distinctive characteristics of the material under investigation, such as the weight of the molecules, maximum dimension (D_{max}) radius of gyration (R_g), and distance distribution function $p(r)$. To measure the flexibility of a protein, the Kratky plot is typically used to qualitatively detect disordered states and differentiate them from spherical proteins. The Kratky representation may show certain aspects of scattering profiles, allowing for simpler detection of the folding state.[16]

The impact of resveratrol on the conformation of various SIRT1•substrate complexes will be investigated using SAXS. In this thesis, we anticipated that resveratrol will drive SIRT1 towards a more compact conformation in situations where it functions as an activator, and inversely in situations where it acts as an inhibitor.

Research goal is to dissect the mechanism of the substrate-dependent regulation of SIRT1 by resveratrol by probing enzyme kinetics, binding interactions, thermal stability, and conformational changes.

2 METHODS

2.1. Protein Expression and Purification

2.1.1. Introduction

A SIRT1-143 construct was utilized in our biochemical studies, which was developed based on previous work.[8] This construct contains the SBD and catalytic core, along with the C-terminal ESA (Essential for Sirtuin Activity) domain (Figure 2.1).

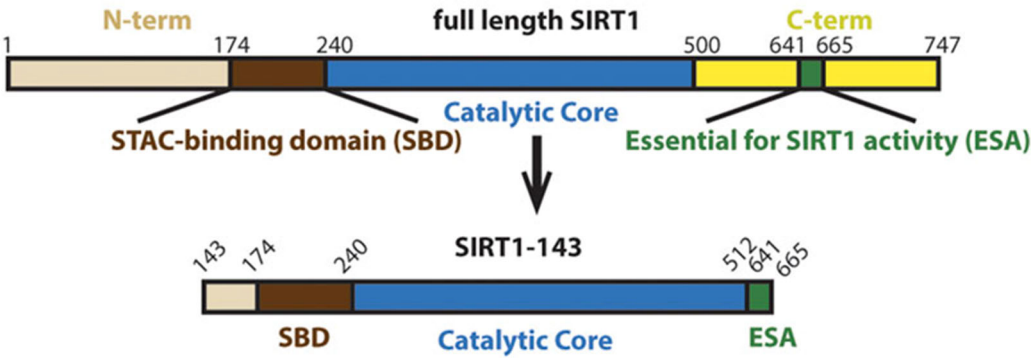

Figure 2.1. Schematic representation of the SIRT1-143 design, which comprises residues 143–512 and the region 641–665.

2.1.2. Methods

A culture that had been grown overnight was diluted 1:100 (v/v) into 0.5-1 liters of Terrific Broth that included 35 ug/mL of Kanamycin. The culture was incubated at 37°C and 220 rpm until Abs600 was close to 0.70, and then induced with isopropyl-1-thio-D-galactopyranoside (IPTG) at a final concentration of 1 mM. The culture was then shaken at 250 rpm for 16 to 18 hours at 16 °C. The cells were collected after 15 minutes of 4,500 x g centrifugation and kept as a dry cell pellet at -80 °C.

The cell pellet was thawed, homogenized, and lysed by sonication in lysis buffer (50 mM Tris pH 8.0, 150 mM NaCl, 20 mM imidazole, 10% glycerol, 100 µM PMSF, and 3 mM β-

mercaptoethanol) and centrifuged at 20,000 rcf for 20 minutes at 4°C in order to clarify the lysate. After equilibration with lysis buffer, the Ni-NTA resin was incubated with the cleared lysate. After incubation, 15 column volumes (CV) of wash Buffer (10% glycerol, 50 mM Tris pH 8.0, 300 mM NaCl, 20 mM imidazole, 3 mM β-mercaptoethanol) were used for washing the resin. Elution buffer, which consists of 50 mM Tris pH 8.0, 150 mM NaCl, 200 mM imidazole, 10% glycerol, and 3 mM beta-mercaptoethanol, was used to elute the His-SUMO-hSIRT1 protein. Ulp1 (a SUMO protease) was added to the combined protein elution fractions in order to cleave off the SUMO-tag. The solution was then dialyzed overnight at 4°C in lysis buffer. By using Size Exclusion Chromatography (SEC) (Hiprep 16/20 Sephacryl S-160), the cleaved hSIRT1 was separated and eluted with storage buffer (50 mM Tris pH 8.0, 150 mM NaCl, 10% glycerol, and 1 mM DTT). SDS-PAGE identified fractions that contained monomeric, cleaved hSIRT1-143, these fractions were mixed, aliquoted, and flash frozen using liquid nitrogen and stored at -80°C. Protein concentration was determined using the BCA and Bradford assays.

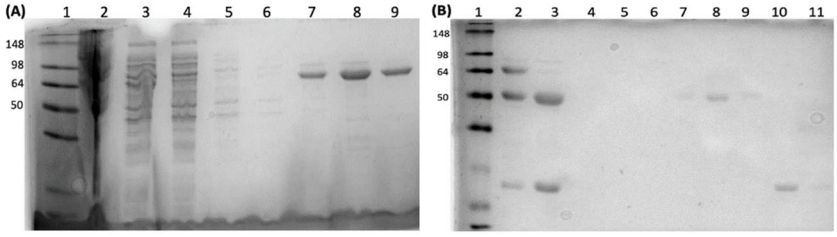

Figure 0.2. SDS-PAGE gels of SIRT1-143. (A) Coomassie Blue stained SDS-PAGE gel of hSIRT1-143 with SUMO tag: Lane 1: SeeBlue^{TM} Plus2 Pre-stained Protein Standard; Lane 2: Insoluble Lysate; Lane 3: Soluble Lysate; Lane 4: Flowthrough; Lane 5: Wash 1; Lane 6: Wash 2; Lane 7: Elution 1; Lane 8: Elution 2; Lane 9: Elution 3. (B) Coomassie Blue stained SDS-PAGE gel following purification using an SEC column and the cleavage of the SUMO solubility tag: Lane 1: SeeBlueTM Plus2 Pre-stained Protein Standard; Lane 2: Pre-cleavage; Lane 3: Post-cleavage; Lane 4: Fraction 10; Lane 5: Fraction 11, Lane 6: Fraction 12, Lane 7: Fraction 15, Lane 8: Fraction 16, Lane 9: Fraction 17, Lane 10: Fraction 19 Lane 11: Fraction 20. hSIRT1-143 is at 46 kDa.**2.2. Enzyme-Coupled Assays**

2.2.1. Introduction

SIRT1 catalyzes protein deacetylation by using NAD^+ as a cosubstrate, resulting in the production of nicotinamide, deacetylated protein, and OAADPr as reaction products. The measurement of nicotinamide production rate, which reflects SIRT1 activity rate, is conducted using a coupled enzyme assembly consisting of nicotinamidase and glutamate dehydrogenase. The enzyme nicotinamidase catalyzes the hydrolysis of nicotinamide, resulting in the formation of nicotinic acid and ammonia. The enzyme glutamate dehydrogenase catalyzes the conversion of ammonia, α-ketoglutarate, and NADPH into glutamate and $NADP^+$ (Figure 2.3).[17] The concentration of NADPH can be calculated using its extinction coefficient at 340 nm, and the rate of the last reaction can be calculated. As the first reaction catalyzed by SIRT1 is the rate limiting step, the rate of NADPH depletion directly reflects the rate of SIRT1 activity.

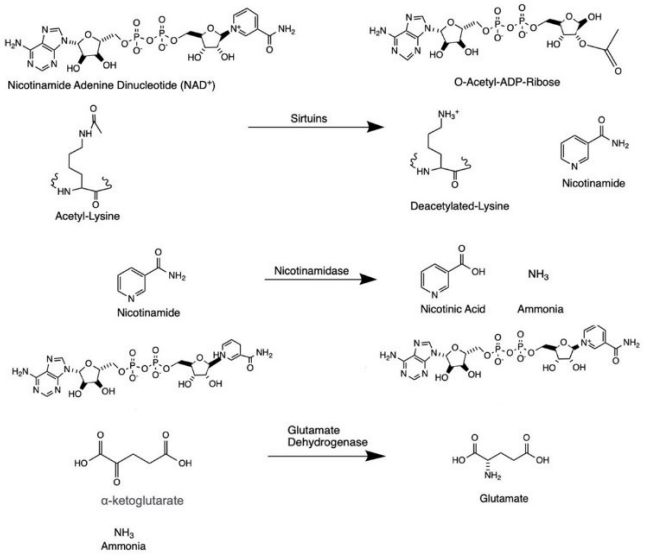

Figure 0.3. Mechanism of the enzyme-coupled assay for nicotinamidase and glutamate dehydrogenase.[17]The enzyme-coupled assays have the qualities of being rapid, cost-effective, precise, and a safer method for determining steady-state kinetic parameters, or the Michaelis-Menten kinetics parameters. The concept referred to as Michaelis-Menten kinetics was postulated by Leonor Michaelis and Maud Leonora Menten in order to explain the kinetics of enzyme reactions. The model elucidates the mechanism by which an enzyme facilitates the acceleration of reaction rates, while also highlighting the influence of enzyme and substrate concentrations on these rates.[18]

The assays have shown their suitability for conducting high-throughput investigations of acetylated substrates or inhibitors, as evidenced by their effective use in a microplate format. Although the coupled assay may exhibit susceptibility to biases resulting from the inhibition

of nicotinamidase or glutamate dehydrogenase, it presents a significant advantage in enabling the continuous monitoring of product generation over a specific duration. Hence, this particular linked assay demonstrates a high level of suitability for conducting high-throughput screening in the search for small-molecule SIRT1 regulators. Furthermore, this assay has the potential to function as a supplementary method for confirming the efficacy of SIRT1 regulators identified by high-throughput screening.[17]

2.2.2. Methods

Measurements were performed to investigate the Michaelis-Menten kinetics of SIRT1 towards different acetylated peptide substrates with and without the addition of resveratrol according to a previous study.[17] The following substances were included in the sample mixtures: 5 - 640 µM of peptide substrate, 640 µM of NAD+, 2 mM of MBP-PncA (nicotinamidase), 20 mM of phosphate buffer at pH 7.6, 3 mM of α-ketoglutarate, 1 mM of DTT, 0.2 mM of NADPH, and 6.7 units of glutamate dehydrogenase. The reactions were initiated by adding 0.2 - 1 µM of the SIRT1 enzyme. SIRT1 reactions were conducted with a final volume of 150 µl per well in a 96-well, transparent, flat-bottomed plate. First, a static reading was taken to assure that the absorbance at 340 nm was stable. 10 minutes after the addition of SIRT1, the absorbance at 340 nm was measured to determine the rate of NADPH depletion. Using 6.22 $mM^{-1}cm^{-1}$ as the extinction coefficient for NADPH and fitting the slope of the linear component of the reaction, the initial rates of the reaction were calculated. As a background control, the initial velocity of the reaction without the peptide substrate was subtracted from the initial velocities of all other reactions. k_{cat} and K_M were determined by fitting the initial rate data to the Michaelis-Menten equation in GraphPad Prism.

2.3. Small Angle X-ray Scattering Experiments

2.3.1. Introduction

The biophysical technique known as small-angle X-ray scattering (SAXS) is used to investigate the overall conformation and structural changes of biological macromolecules while they are in a solution.[16] In a SAXS experiment, a collimated, monochromatic X-ray beam with an energy range of ~7–13 keV is directed at the sample. A ion beam is generated by a synchrotron —a specific type of cyclic particle accelerator—, and then deflected by a wiggler. The wiggler deflects the beam and slows down the particle, converting its kinetic energy into electromagnetic radiation and generating an x-ray beam.[19] The X-ray beam strikes the protein and disperses at low angles (typically a few degrees). The resultant x-ray patterns are recorded using a detector, and analyzed to determine structure transitions.

The ability to exhibit flexibility across different domains of proteins is often essential for proper functioning. The investigation of movements of proteins that exhibit significant flexibility on a broad scale is typically challenging using standard structural techniques such as X-ray crystallography or electron microscopy where the protein is immobile. The collection of SAXS data has shown to be compatible with high throughput methods, and there has been a notable improvement in the quality of data obtained from samples with low concentrations, which is below 1 mg/ml.[20]

2.3.2. Method

SAXS was used to examine the effect of resveratrol on the conformation of the various SIRT1•substrate complexes. 40 μM of hSIRT1-143 was diluted in storage buffer (50 mM Tris pH 8.0, 150 mM NaCl, 1 mM DTT) to produce SAXS samples. Except for the sample

containing apo SIRT1, all other samples contained 640 μM Adenosine diphosphate ribose (ADPr) which is an NAD^+ analog. The various samples were supplemented with peptide substrates at concentrations ranging from 500 to 5000 μM. Based on previous kinetics assays, the final concentration of peptide substrate was calculated to ensure that SIRT1 is largely saturated with the peptide. To the "+ Resveratrol" samples, 200 μM resveratrol was added.

At the Lawrence Berkeley National Laboratory (CA, USA), SAXS data were collected utilizing the Advanced Light Source SIBYLS beamline12.3.1 in high-throughput mode (HT-SAXS). With an X-ray wavelength of 1.216 Å and a distance of 2070 mm between the sample and detector, the scattering vector, q, ranged from 0.01 to 0.45. Where 2θ represents the angle of scattering, the scattering vector is defined as $q=4\pi \sin \theta/\lambda$. Experiments were performed at a temperature of 20°C. Using the SAXS FrameSlice program (https://bl1231.als.lbl.gov/ran), the sample was deposited for 10s with detector framing at 0.3s to improve the signal. Utilizing Primus, the combined SAXS profile was plotted. Utilizing ATSAS 3.0 Primus software, the combined SAXS was plotted and analyzed.

2.4. Differential Scanning Fluorimetry

2.4.1. Introduction

Differential scanning fluorimetry (DSF) is a cost-effective and efficient method for determining the melting temperature (T_{Ma}) of a protein sample, which in turn reflects the protein's thermal stability. In a DSF experiment, a sample is subjected to thermal treatment, and its denaturation process is assessed by measuring its interaction with a solvatochromic dye that emits fluorescence, such as SYPRO® Orange. The experiment involves subjecting

the protein to heat denaturation, which leads to the exposure of the hydrophobic core of the protein. This exposure causes an increase in fluorescence intensity when the SYPRO® Orange dye binds to these exposed hydrophobic areas. The decline in fluorescence signal subsequent to the melting transition is often ascribed to the depletion of hydrophobic regions that interact with SYPRO® Orange during protein aggregation at elevated temperatures.[21] Recently, it has been shown that this particular approach is appropriate for applications characterized by low volume and high throughput.[22]

2.4.2. Method

To quantify the effect of resveratrol on the thermal stability of the different SIRT1•substrate complexes, differential scanning fluorimetry (DSF) was used. DSF experiments were conducted in a 384-well plate using an Analytik Jena qTOWER real-time PCR thermal cycler. In "Normal" mode, the fluorescence intensity was recorded in the TAMRA channel (Ex: 535nm Em: 580nm) over one hour with a 1°C increase in temperature per cycle. Each well contained 25 μM hSIRT1 bound to a surplus of ADPr (640 μM), 200 μM resveratrol, and 500 – 5000 μM peptide substrate (as determined by kinetic data for each condition). In addition, a buffered SYPRO® Orange (Millipore) dye dilution of 1:100 was added to each well. For all conditions, buffer-only controls containing ADPR, resveratrol, and peptide were measured in triplicate. T_{Ma} was determined in GraphPad Prism using the first derivative method and Lorentzian distribution fitting to the first derivative curve (T_{Ma} = center of curve/inflection point).[23]

2.5. Binding Affinity Measurements

2.5.1. Introduction

Tryptophan fluorescence quenching is a fluorescence spectroscopy technique often used in binding affinity measurements. The measurement depends on the capacity to suppress the intrinsic fluorescence of tryptophan residues (Ex=280nm Em= approx. 350 nm) present in SIRT1. This change in fluorescence is caused by changes in the polarity of the surrounding atmosphere experienced by the residues upon the presence of a change in the protein, such as binding to a ligand. Quenching may occur as a result of localized alterations in the vicinity of the interaction site or due to conformational changes caused by binding. Considerable quenching may also occur in situations when the titrant absorbs at or in close proximity to the excitation or emission wavelengths of tryptophan.[24]

As both tryptophan residues in the SIRT-143 construct are located in the SBD (Figure 2.4), where resveratrol is shown to bind[1], intrinsic tryptophan fluorescence quenching assays were utilized to quantify the binding affinity between resveratrol and the different SIRT1•substrate complexes.

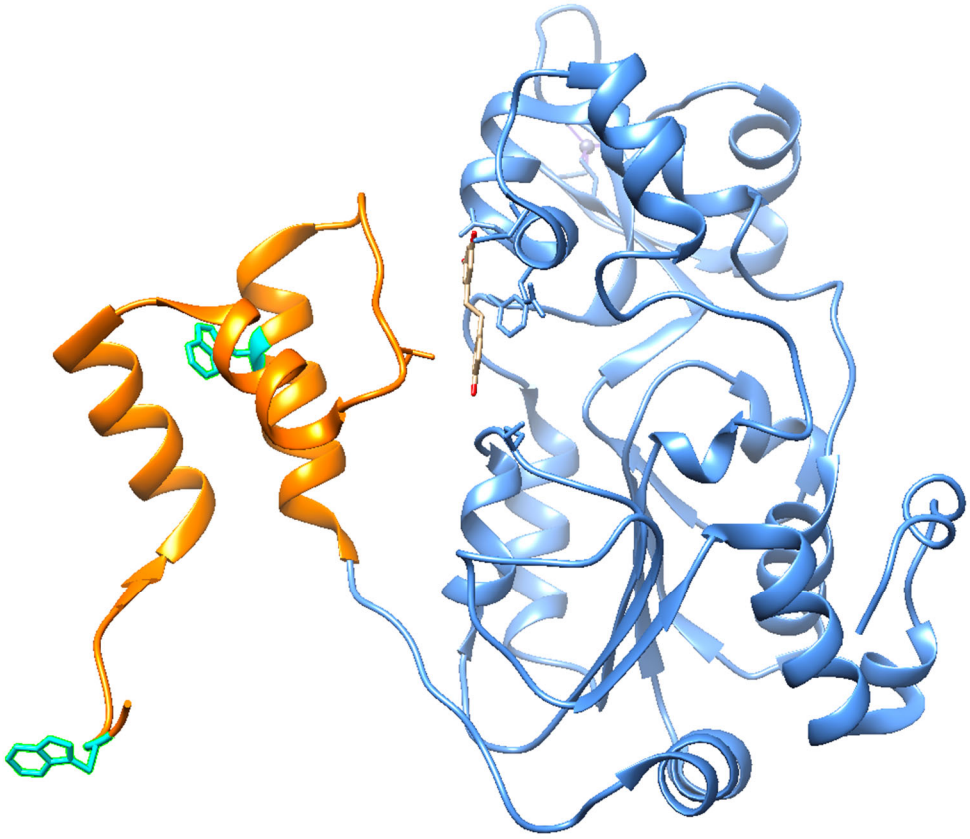

Figure 0.4. The SIRT-143 structure has two tryptophan residues (cyan), both of which are in the SBD (orange).**2.5.2. Method**

Resveratrol was titrated into a quartz cuvette containing 150 µl of 2 µM SIRT1-143 (20 mM phosphate buffer, pH 7.6) at concentrations ranging from 0.7 to 422.6 µM. The intensity of intrinsic tryptophan fluorescence was determined utilizing a Cary Eclipse Fluorescence Spectrometer with excitation at 285 nm and emission between 300 and 500 nm. The intensity of fluorescence was detected at the peak of the emission spectrum (330-337 nm). Fluorescence intensity (F_i) was changed such that $\Delta F = F_0 - F_i$ to adjust for dilution effects and background fluorescence from the hSIRT1 protein (F_0). A 1:1 binding model of hSIRT1

to resveratrol was utilized in GraphPad Prism to ascertain the apparent equilibrium dissociation constant (K_D). The observed increase in fluorescence fraction ($\Delta F/F_0$) was depicted as a function of resveratrol concentration, and a binding isotherm that reflects ligand depletion (equation 2.1) was applied. The parameters a and x represent the total concentrations of SIRT1-143 and resveratrol, respectively. y represents the observed relative fluorescence quenching at any resveratrol concentration. b and c represent the maximum and minimum observed relative fluorescence quenching values, respectively.

$$y = c + (b - c) \times \frac{((K_D + a + x) - \sqrt{(K_D + a + x)^2 - 4 \times a \times x})}{2 \times a} \quad (2.1)$$

3 RESULTS

3.1. Resveratrol Induces Changes in the K_M of SIRT1 Under Conditions of both Activation and Inhibition

The previous studies that characterized resveratrol as a dual inhibitor and activator mostly used end-point assays. We carried out enzyme kinetics studies modeled on previous work to deepen our understanding of the allosteric regulatory mechanism.[17] These assays were performed to determine the Michaelis-Menten parameters for SIRT1's activity against various peptide substrates, both in the presence and absence of resveratrol (Figure 3.1). Among the five peptide substrates selected based on prior research, we found that resveratrol enhanced overall SIRT1 activity (k_{cat}/K_M) towards Ac-p53W by 2-fold and lowered overall SIRT1 activity towards Ac-p53, Ac-H4, Ac-H3, and Ac-CSNK by 30%-50% (Table 3.1).[12] Resveratrol affected SIRT1 differently when different substrates were involved. The following experiments were conducted to determine whether resveratrol interacts differently with the SIRT1 substrate complex regarding its thermal stability.

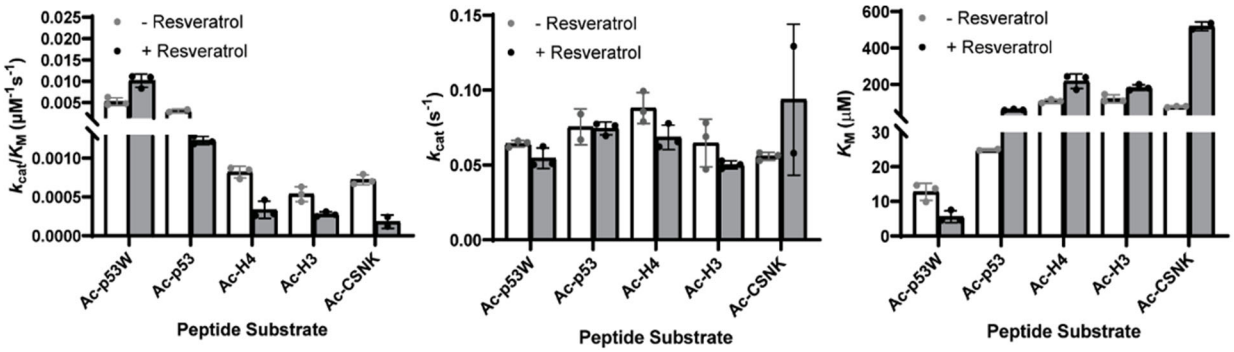

Figure 0.1. Michaelis-Menten parameters for SIRT1 activity against different peptide substrates with and without resveratrol.

Table 0.1.
Michaelis-Menten Kinetic Parameters for SIRT1-143 Activity Towards Various Acetylated Peptide Substrates with and without the Addition of Resveratrol (200 μM)

Peptide Substrates	Resveratrol	k_{cat} (s^{-1})	K_M (μM)	k_{cat}/K_M ($\mu M^{-1}s^{-1}$)
Ac-p53W (STSRHKK^{Ac}WMFKTE)	-	0.06 ± 0.001	13 ± 1.4	0.005 ± 0.0005
	+	0.06 ± 0.004	6 ± 1.0	0.01 ± 0.0009
Ac-p53 (STSRHKK^{Ac}LMFKTE)	-	0.08 ± 0.009	25 ± 0.2	0.003 ± 0.00003
	+	0.07 ± 0.002	61 ± 1.6	0.002 ± 0.0003
Ac-H4 (VRGKAGK^{Ac}GLGKGG)	-	0.09 ± 0.006	108 ± 5.5	0.001 ± 0.0004
	+	0.07 ± 0.005	217 ± 23.2	0.0005 ± 0.0001
Ac-H3 (KSTGGK^{Ac}APRKQ)	-	0.06 ± 0.009	121 ± 12.6	0.0005 ± 0.0003
	+	0.05 ± 0.002	183 ± 8.9	0.0003 ± 0.00006
Ac-CSNK (ASSSGSK^{Ac}AEFIVG)	-	0.06 ± 0.002	78 ± 2.2	0.0007 ± 0.0002
	+	0.09 ± 0.036	519 ± 16.9	0.0005 ± 0.0001

Note. All data on enzyme kinetics were collected in triplicates or duplicates. The Michaelis-Menten parameters were fitted using GraphPad Prism, and the average and standard deviation were provided. Between — resveratrol and + resveratrol samples, all K_M and k_{cat}/K_M values had a p-value < 0.05. p-value was > 0.05 difference for k_{cat} values between —resveratrol and + resveratrol samples.

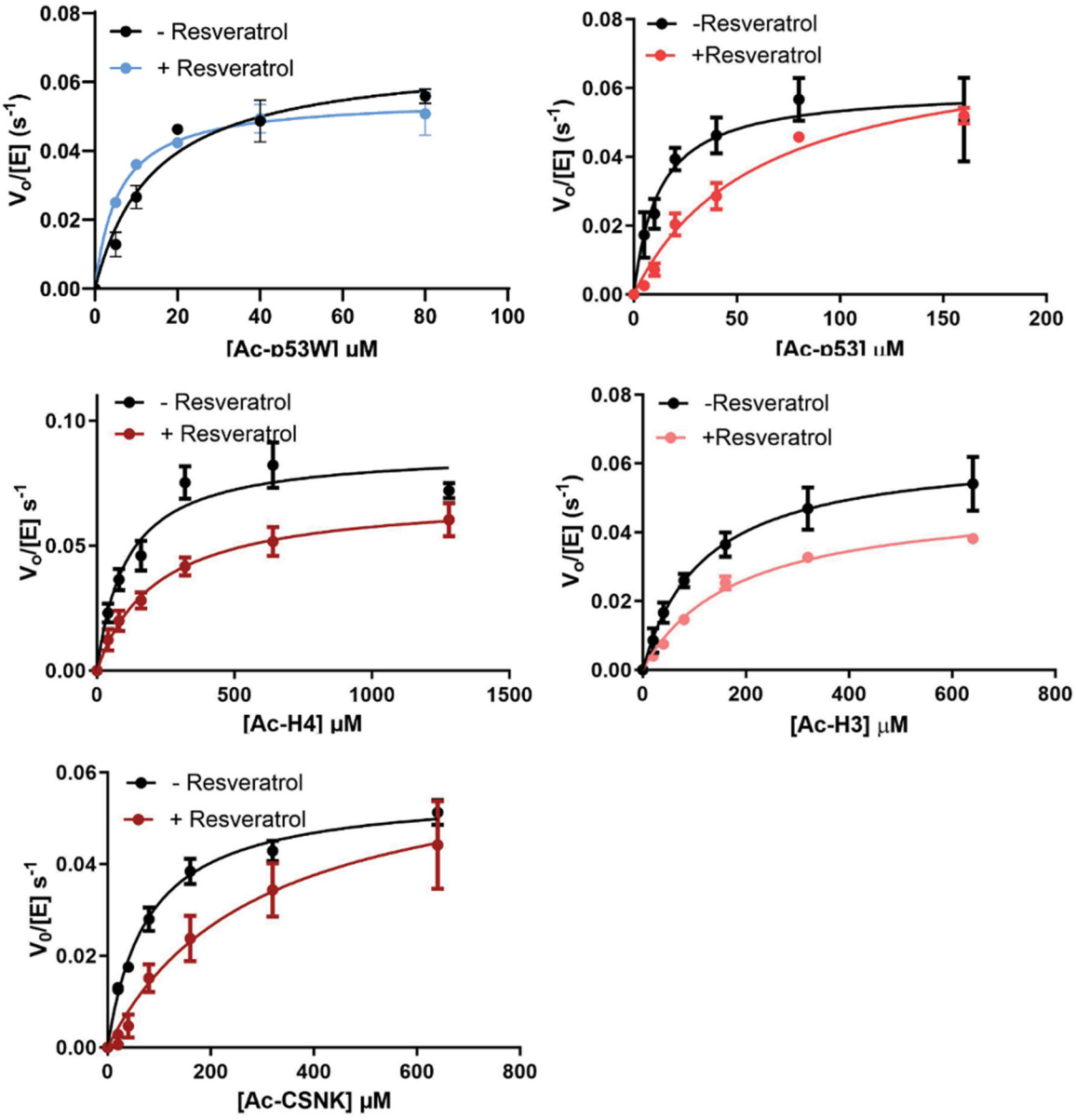

Figure 0.2. SIRT1 enzyme kinetics curves against Ac-p53W, Ac-p53, Ac-H3, Ac-H4, and Ac-CSNK with and without the presence of resveratrol.**3.2. Resveratrol Reduces SIRT1's Thermal Stability to a Greater Extent in Inhibitory Situations**

To assess the influence of resveratrol on the thermal stability of different SIRT1•substrate complexes, we employed differential scanning fluorimetry (DSF) using SYPRO® Orange as the dye.[23] We used ADPr (Adenosine diphosphate ribose), an analog of NAD^+, a cosubstrate

of SIRT1, in addition to the peptide substrate. The first derivative approach for determining T_{ma} was used to obtain the melting temperatures (Figure 3.3). This made it possible to compare the relative T_{ma} values for different SIRT1•substrate complexes with and without resveratrol.

The apo hSIRT1-143's T_{ma} value was 51.1°C ± 0.3°C, which is within the range observed in other research.[25] Resveratrol, whether acting as an activator or inhibitor (ΔT_{ma} = 1°C–4°C, individually), generally destabilized apo SIRT1, SIRT1 in combination with only ADPr, and all of the SIRT1•substrate complexes (Table 3.2). Nevertheless, the impact of resveratrol on the stability of SIRT1 complexes in the presence of inhibitory conditions (Ac-p53, Ac-H4, Ac-H3, and Ac-CSNK) was more severe resulting in a decrease in the melting temperature by 2°C–4°C. Conversely, when resveratrol acted as an activator in the SIRT1•ADPR•Ac-p53W complex, it only caused a reduction in the melting temperature by 1°C. Resveratrol lowered the T_{ma} of apo SIRT1 by 1.7°C in the absence of substrate, but only by 0.2°C in the presence of ADPr. It is possible that resveratrol influences SIRT1 stability, and that ADPr "protects" resveratrol from destabilizing the protein, but that the addition of peptide substrates render SIRT1 less rigid or vulnerable to resveratrol-induced instability. This experiment gave us information on how resveratrol affects SIRT1 stability, we wanted to get a more complete picture and directly look at how resveratrol affects the conformation of SIRT1 as well.

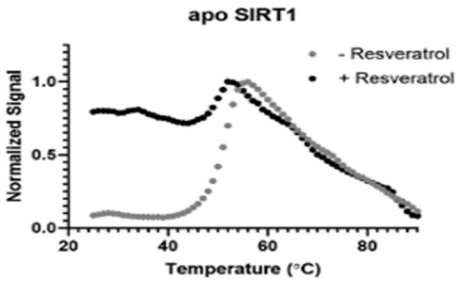
apo SIRT1
- Resveratrol
+ Resveratrol
Normalized Signal
1.0
0.5
0.0
20
40
60
80
Temperature (°C)

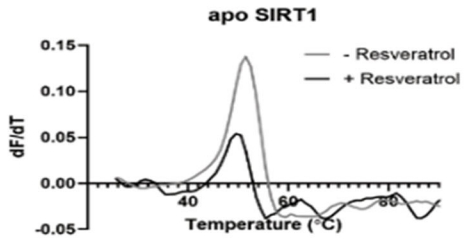
apo SIRT1
- Resveratrol
+ Resveratrol
dF/dT
0.15
0.10
0.05
0.00
-0.05
40
60
80
Temperature (°C)

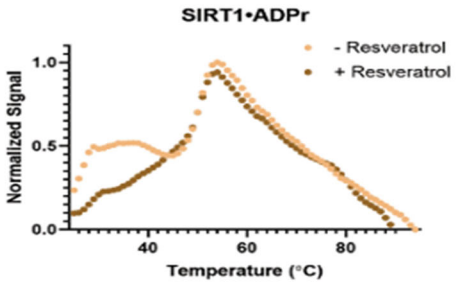
SIRT1•ADPr
- Resveratrol
+ Resveratrol
Normalized Signal
1.0
0.5
0.0
40
60
80
Temperature (°C)

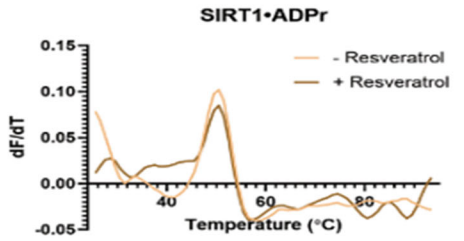
SIRT1•ADPr
- Resveratrol
+ Resveratrol
dF/dT
0.15
0.10
0.05
0.00
-0.05
40
60
80
Temperature (°C)

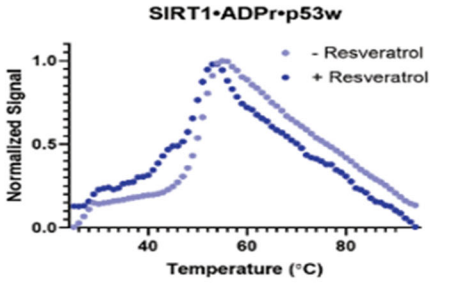
SIRT1•ADPr•p53w
- Resveratrol
+ Resveratrol
Normalized Signal
1.0
0.5
0.0
40
60
80
Temperature (°C)

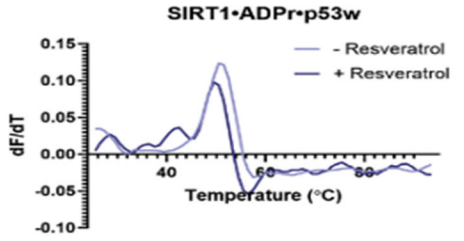
SIRT1•ADPr•p53w
- Resveratrol
+ Resveratrol
dF/dT
0.15
0.10
0.05
0.00
-0.05
-0.10
40
60
80
Temperature (°C)

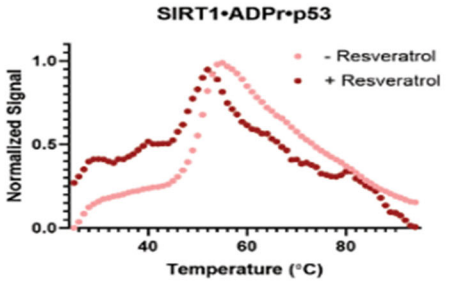
SIRT1•ADPr•p53
- Resveratrol
+ Resveratrol
Normalized Signal
1.0
0.5
0.0
40
60
80
Temperature (°C)

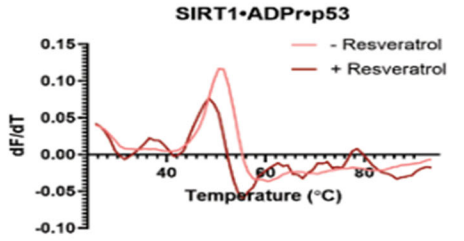
SIRT1•ADPr•p53
- Resveratrol
+ Resveratrol
dF/dT
0.15
0.10
0.05
0.00
-0.05
-0.10
40
60
80
Temperature (°C)

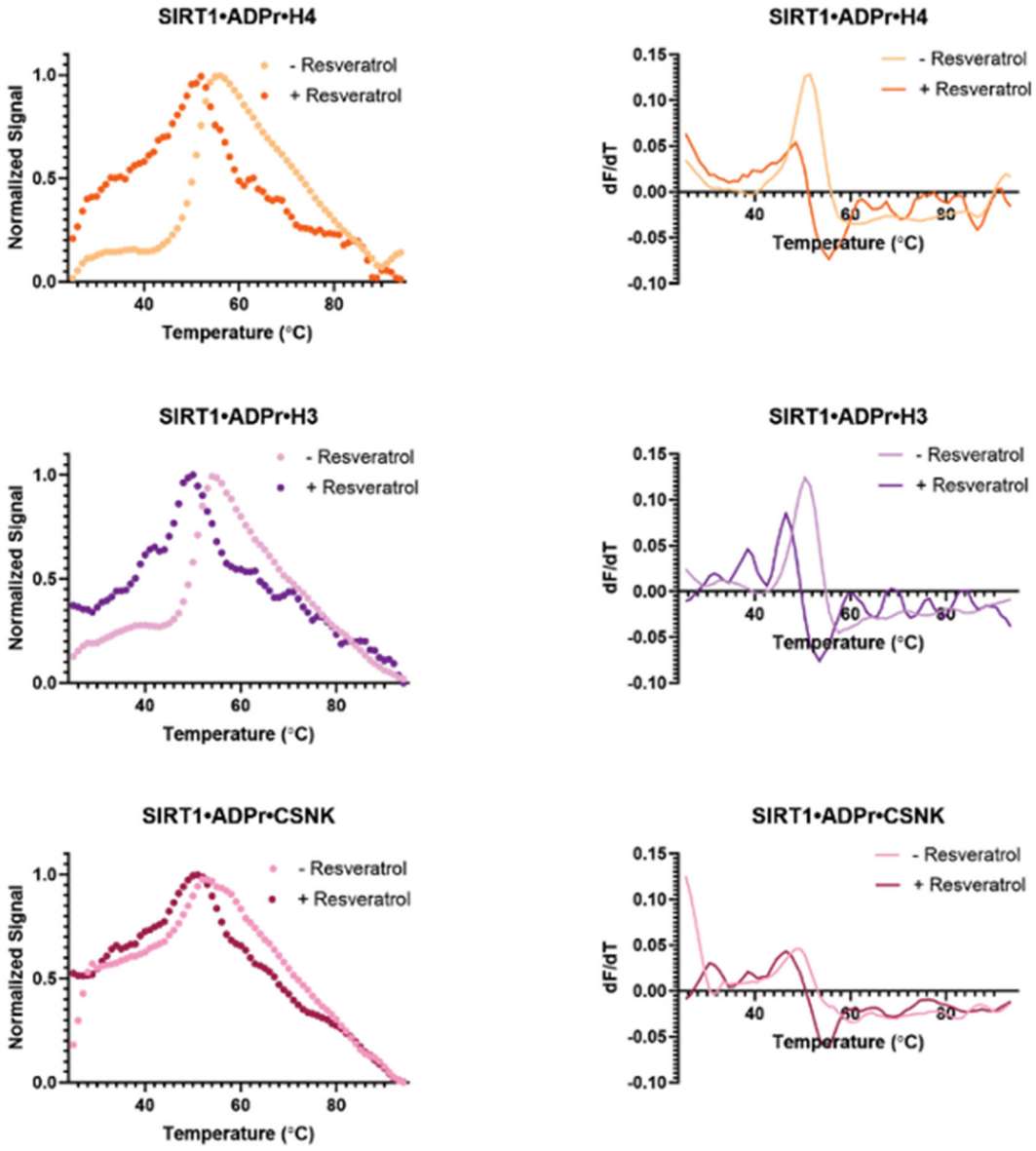

Figure 0.1. DSF melting curves and first derivatives for apo SIRT1 and SIRT1•substrate complexes with and without resveratrol addition. Resveratrol stimulates SIRT1 activity towards Ac-p53W while inhibiting SIRT1 activity towards Ac-p53, Ac-H3, Ac-H4, and Ac-CSNK.

Table 0.1.
The Melting Temperatures of SIRT1, When Combined with Various Peptide Substrates and ADPr (an analog of NAD^+), were Determined

Protein Complex	T_{ma} (°C) - Res	T_{ma} (°C) + Res
apo SIRT1	51.1 ± 0.27	49.4 ± 0.48
SIRT1•ADPr	50.1 ± 0.34	49.9 ± 0.44
SIRT1•ADPr•Ac-p53W	50.7 ± 0.27	49.5 ± 0.46
SIRT1•ADPr•Ac-p53	50.6 ± 0.009	48.2 ± 0.54
SIRT1•ADPr•Ac-H4	50.9 ± 0.26	46.5 ± 1.49
SIRT1•ADPr•Ac-H3	50.4 ± 0.32	46.3 ± 0.55
SIRT1•ADPr•Ac-CSNK	48.2 ± 0.57	46.0 ± 0.94

Note. The data was analyzed by fitting the first derivative of the differential scanning fluorimetry (DSF) data using a Lorentzian function. Additionally, the effects of adding 200 μM resveratrol were examined. Data are typically gathered in triplicate or duplicate to ensure accuracy and reliability. However, it should be noted that the SIRT1•ADPr•Ac-H3 + Resveratrol data set consists of just a single data set. The SEM of fit and the curve's center/inflection point are provided.

3.3. Resveratrol Alters SIRT1 Conformation in Different Ways in Activation and Inhibition Scenarios

We used small angle X-ray scattering (SAXS) to investigate the impact of resveratrol on SIRT1 conformation in the presence of various peptide substrates. In brief, SIRT1 was complexed with ADPr as well as the various peptide substrates at saturating concentrations with SIRT1 based on information from our kinetic data. SAXS profiles were collected for these complexes with and without the addition of 200 μM resveratrol. To confirm that the SAXS results solely represented the conformation of SIRT1 and not the free peptide substrates, a "blank" solution containing all components in the samples (substrates, resveratrol, etc.) except SIRT1 was utilized for background subtraction. SIRT1 was shown to be monomeric in all samples according to molecular weight analysis.[26] The obtained SAXS profile of apo SIRT1, along with the SAXS profiles of other SIRT1 complexes, exhibited notable dissimilarities when compared to the calculated SAXS profile of SIRT1-143 based on the X-ray crystal structure (which notably does not represent SIRT1 in solutions). This

calculation was performed using the PDB structure 5BTR and the FOXS web server.[27] The anticipated radius of gyration (R_g) for SIRT1-143 based on the crystal structure is 23 Å. However, the observed R_g values in experimental studies were consistently more than 30 Å. This indicates that in a solution environment, the conformation of SIRT1 is much more extended compared to its tightly folded structure seen in crystal form. Furthermore, the small-angle X-ray scattering (SAXS) results indicate that SIRT1 adopts a conformation resembling a rod, with a radius of gyration varying from 31 - 37 Å and a radius of cross-section (R_{xs}) varying from 10 - 14 Å. The p(r) function illustrates the distribution of distances between pairs of points within the particle.[20] This analysis reveals that the particle exhibits a predominantly compact conformation with a diameter of approximately 30-35 Å. However, there is also a minor population of SIRT1 that adopts an extended conformation with a diameter exceeding 100 Å (Figure 3.5). This observation aligns with the findings from previous investigations of SIRT1, which have demonstrated the inherent flexibility of the loop connecting the substrate-binding domain (SBD) and the catalytic core with significant fluctuations in conformation relative to the core.[8,1] Furthermore, prior research has indicated that the three helices comprising the SBD may undergo disordering and reduced bundling upon binding with inhibitor proteins.[9]

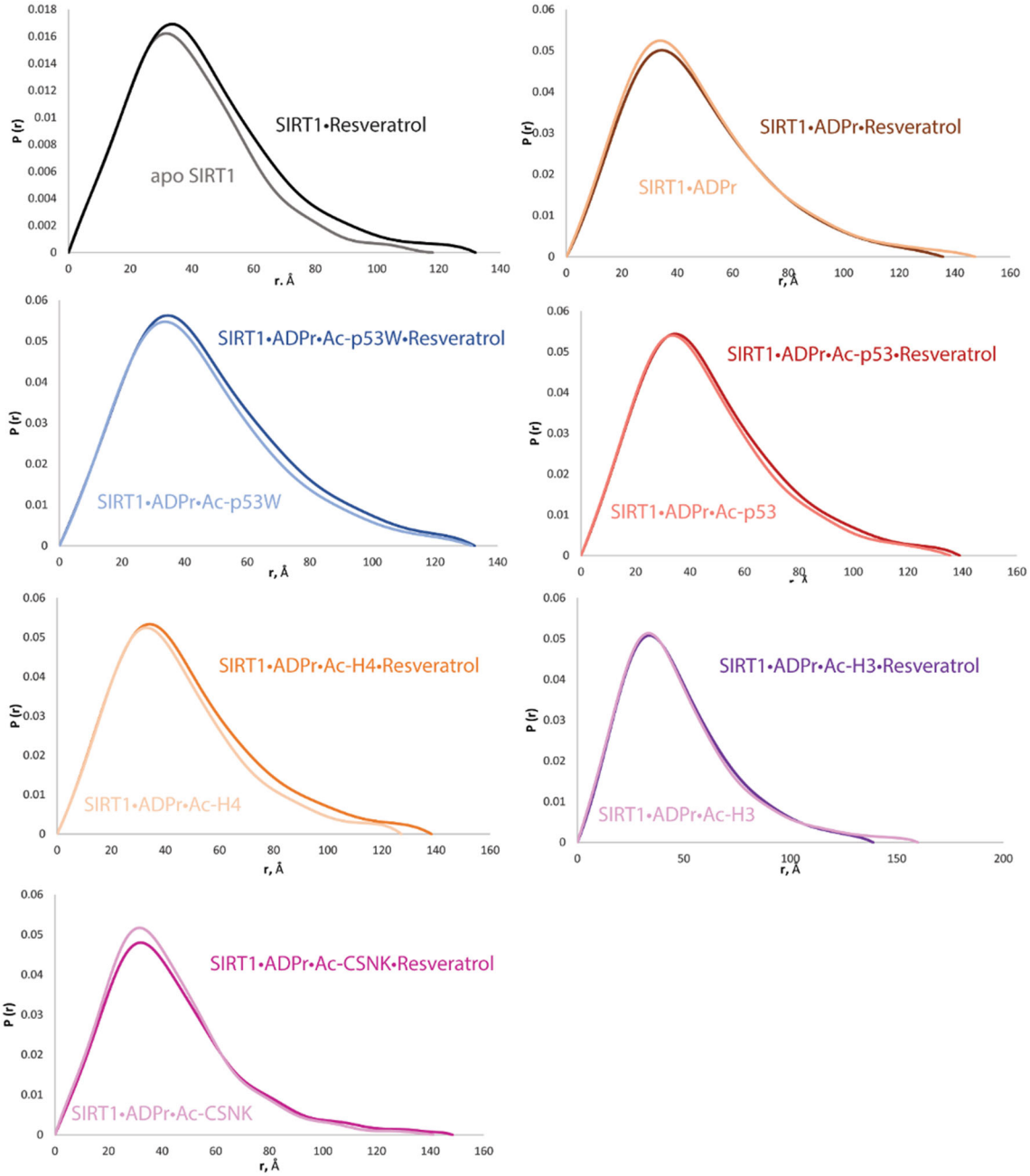

Figure 0.1. P(r) overlay plots from the ATSAS 3.0 Primus program for SIRT1•substrate complexes with and without resveratrol addition. The addition of resveratrol has an impact on the larger population.

Table 0.1.
SIRT1 Conformation in Solution with Peptide Substrates and ADPr, with and without the Addition of 200 M Resveratrol, as Measured using the Advanced Light Source SIBYLS Beamline12.3.1.

Protein Complex	Resveratrol	R_g (Å)	Δ R_g (%)	R_{xs}	Δ R_{xs} (%)
apo SIRT1	-	30.35	6.3%	10.26	9.7%
	+	32.26		11.26	
SIRT1•ADPr	-	34.85	1.7%	10.14	39.9%
	+	35.45		14.19	
SIRT1•ADPr•Ac-p53W	-	33.9	8.9%	12.97	6.9%
	+	36.91		13.86	
SIRT1•ADPr•Ac-p53	-	33.87	9.2%	12.67	22.0%
	+	34.92		14.37	
SIRT1•ADPr•Ac-H4	-	33.88	7.3%	11.23	18.7%
	+	36.99		13.7	
SIRT1•ADPr•Ac-H3	-	34.26	3.1%	11.06	13.4%
	+	35.94		12.42	
SIRT1•ADPr•Ac-CSNK	-	31.58	4.9%	10.67	12.3%
	+	33.87		12.67	

Note. The SAXS data were acquired twice. When Resveratrol is added, all Rg and Rxs values rise, with Rxs increasing at a greater proportion than Rg.

After comparing the SAXS profiles obtained with and without the presence of resveratrol, it became evident that the inclusion of resveratrol resulted in the elongation of the SIRT1 conformation, irrespective of the specific sequence of the peptide substrate (Figure 3.5). However, the observed increase in R_{xs} was greater in percentage (ranging from 12% to 22%) compared to R_g (ranging from 3% to 9%) under conditions where resveratrol functions as an inhibitor (specifically, with substrates Ac-p53, Ac-H4, Ac-H3, Ac-CSNK). In the case of resveratrol acting as an inhibitor, there is a possibility that the cross-section could increase to more than the total volume. Conversely, when SIRT1 was complexed with Ac-p53W, the condition in which resveratrol acts as an activator, R_{xs}, and R_g were raised by a similar percentage (7%) (Table 3.3). There is a possibility that an extended SIRT1

conformation will occur in both Rg and Rxs as a result of greater protein flexibility in the resveratrol-as-activator scenario.

While comparing the p(r) functions obtained in our study, it appears that the inclusion of resveratrol has an impact on the more extended population of SIRT1 with a radius around 100 Å. However, due to the limited size of this particular population in our sample, more comprehensive analysis is impeded by the weak signal to noise ratio observed in this specific region, and more experiments are needed for a concrete conclusion.

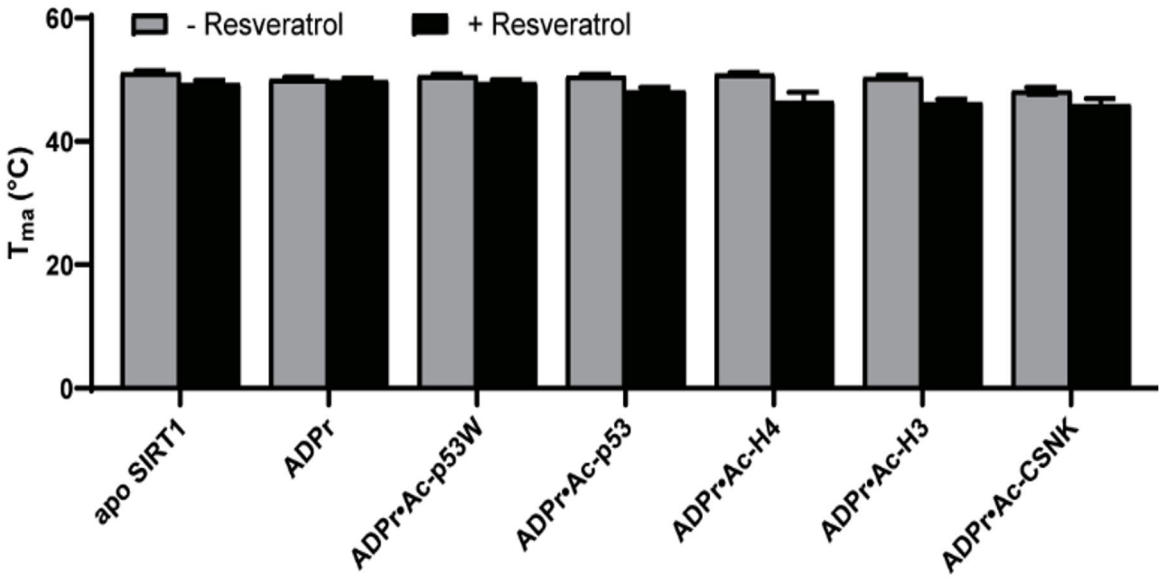

Figure 0.2. Bar graph of T_M values for various SIRT1 complexes with and without the addition of resveratrol. Data are collected in triplicate or duplicate, the SIRT1•ADPr•Ac-H3 + Resveratrol data set is only a single data set. The center of the curve/inflection point and SEM of fit are reported.

3.4. Resveratrol Binds to SIRT1 with a Decreased Affinity in Activation Conditions

Our objective was to provide more elucidation on the underlying mechanism through which resveratrol exhibits dual functionality as both an activator and inhibitor, with a focus

on its interaction with peptide substrates. Prior research has shown that the catalytic core of SIRT1 experiences changes in its conformation upon binding with its substrates.[4]

Our hypothesis suggested that various substrates would elicit distinct conformational alterations, hence resulting in differential interactions with resveratrol. In order to evaluate this, we measured the binding affinity of resveratrol to the different SIRT1•substrate complexes via a tryptophan quenching assay.[24]

The hSIRT1-143 construct has two tryptophan residues, specifically W176 and W221, which are both situated in the SBD area where resveratrol binds. The fluorescence intensity emitted by tryptophan at 330 nm was significantly reduced with the titration of resveratrol (Figure 3.5). This phenomenon facilitated the determination of the binding affinity between the different SIRT1•substrate complexes and resveratrol. The dissociation constant (K_D) values obtained from the experiments are shown in Table 3.4 and Figure 3.6.

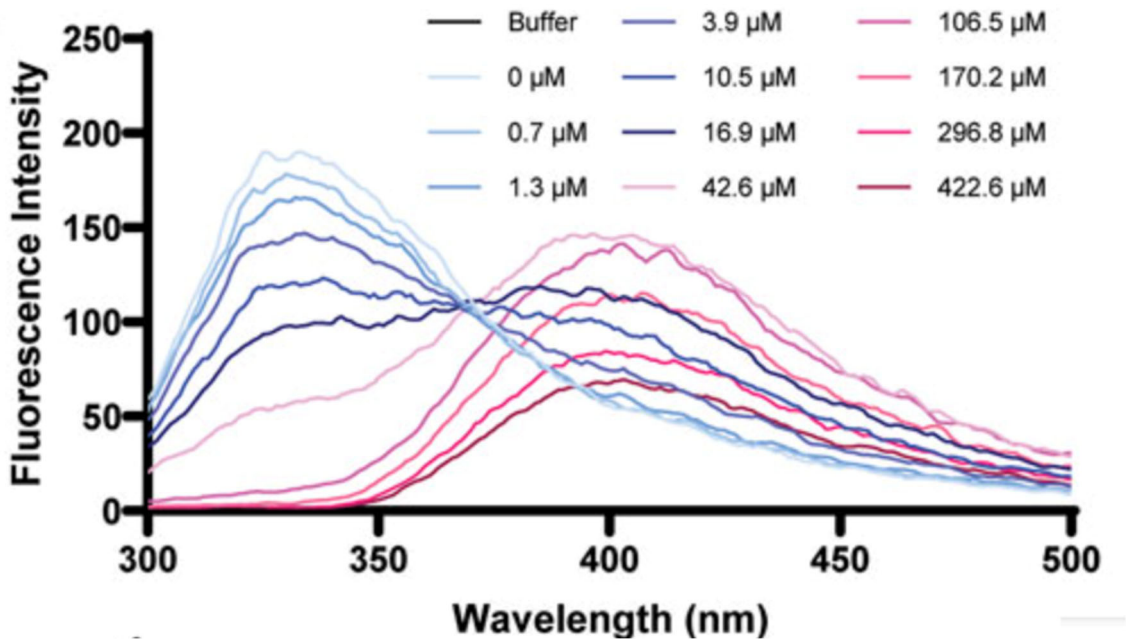

Figure 0.1. Representative fluorescence spectra of SIRT1 upon titration of resveratrol from 0.7 μM to 422.6 μM showing the decrease of the peak at 330 nm.

Table 0.1.

Fluorescence-Based Binding Curves of Resveratrol Binding to SIRT1 in Complex with Different Substrates

Protein Complex	**K_D (μM)**
apo SIRT1	28 ± 3.5
SIRT1•NAD$^+$	19 ± 1.0
SIRT1•ADPr	16 ± 2.3
SIRT1•ADPr•Ac-p53W	78 ± 14.1
SIRT1•ADPr•Ac-p53	16± 6.0
SIRT1•ADPr•Ac-H4	24 ± 1.2
SIRT1•ADPr•Ac-H3	20 ± 3.2
SIRT1•ADPr•Ac-CSNK	28 ± 2.0

Note. Data was fit to ligand depletion binding equation using GraphPad Prism. All measurements were performed in triplicate and the average and SEM are reported. Only the binding affinity of resveratrol to the SIRT1•ADPr•Ac-p53W complex is statistically significant different (p-value < 0.05) from the binding affinity of resveratrol to apo SIRT1.

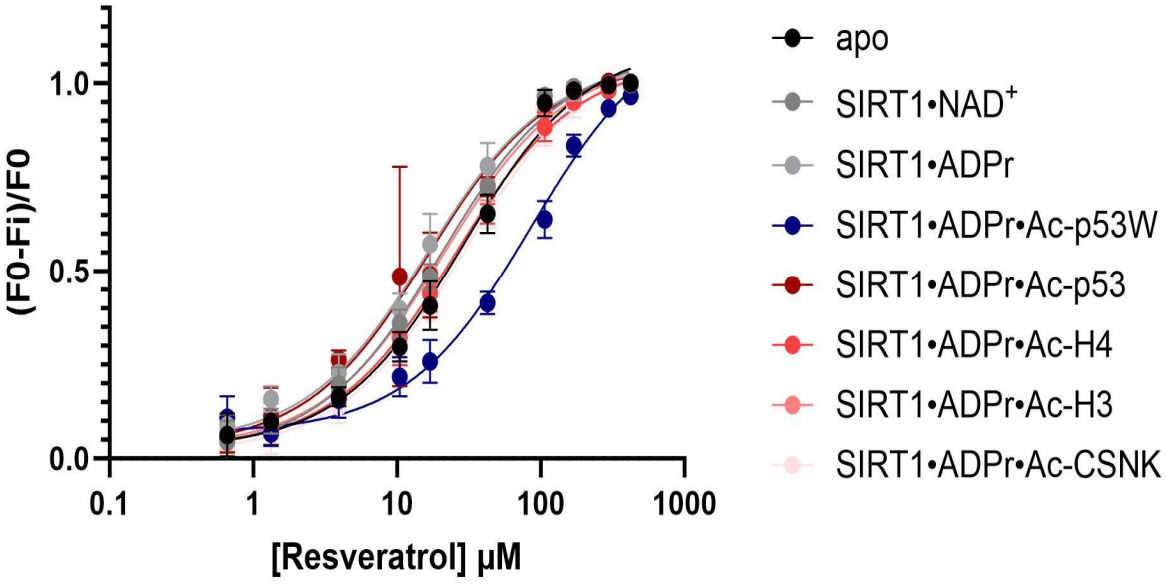
(F0-Fi)/F0
1.0
0.5
0.0
0.1
1
10
100
1000
[Resveratrol] µM
apo
SIRT1•NAD+
SIRT1•ADPr
SIRT1•ADPr•Ac-p53W
SIRT1•ADPr•Ac-p53
SIRT1•ADPr•Ac-H4
SIRT1•ADPr•Ac-H3
SIRT1•ADPr•Ac-CSNK

Figure 0.2. Representative binding isotherms from Graphpad Prism for resveratrol binding to apo SIRT1 and SIRT1 in complex with substrates. Resveratrol acts as an activator for SIRT1 activity towards Ac-p53W and acts as an inhibitor for SIRT1 activity towards Ac-p53, Ac-H3, Ac-H4, and Ac-CSNK.We used ADPr as a non-reacting substitute for NAD^+ in the same way that we did in the DSF and SAXS investigations. The K_D values for resveratrol and SIRT1•NAD^+ and SIRT1•ADPr were similar, indicating that ADPr had the same impact on SIRT1 conformation as NAD^+ and was a close substitute. Our K_D values were similar to those reported in recent investigations using isothermal calorimetry (ITC).[13] The K_D values obtained for resveratrol and apo SIRT1 in our study were measured to be 28 μM, which is a bit lower than the K_D value reported in the literature, which is 50 μM. The observed discrepancy may be attributed to variations in the SIRT1 constructions used. In our study, our construct included residues 143-182, while the construct described in the literature commenced at residue 183. Given the established binding affinity of resveratrol to the SBD region (174–240) as reported by Cao et al. (2015), it is reasonable to hypothesize that the inclusion of an adjacent segment of 40 amino acids might potentially enhance the interaction. The K_D for the interaction between resveratrol and the SIRT1•ADPr•Ac-p53 complex was determined to be 16 μM in our study, which is consistent with the previously reported value of 14 μM in the literature.[13]

Prior research has shown that the interaction intensity between resveratrol and SIRT1 may be modulated by the addition of peptide substrates. Intriguingly, when examining the binding affinity of resveratrol to various SIRT1•substrate complexes, we observed that resveratrol exhibited significantly weaker binding affinity to the SIRT1•ADPr•Ac-p53W complex compared to its binding affinity to the other SIRT1 complexes, which displayed relatively similar affinities for binding (Figure 3.8). Resveratrol bound to SIRT1 differently

with SIRT1•ADPr•Ac-p53W complex. The fastest way to figure it out was prediction software to check the different peptides had changed the conformation of SIRT1 in different ways.

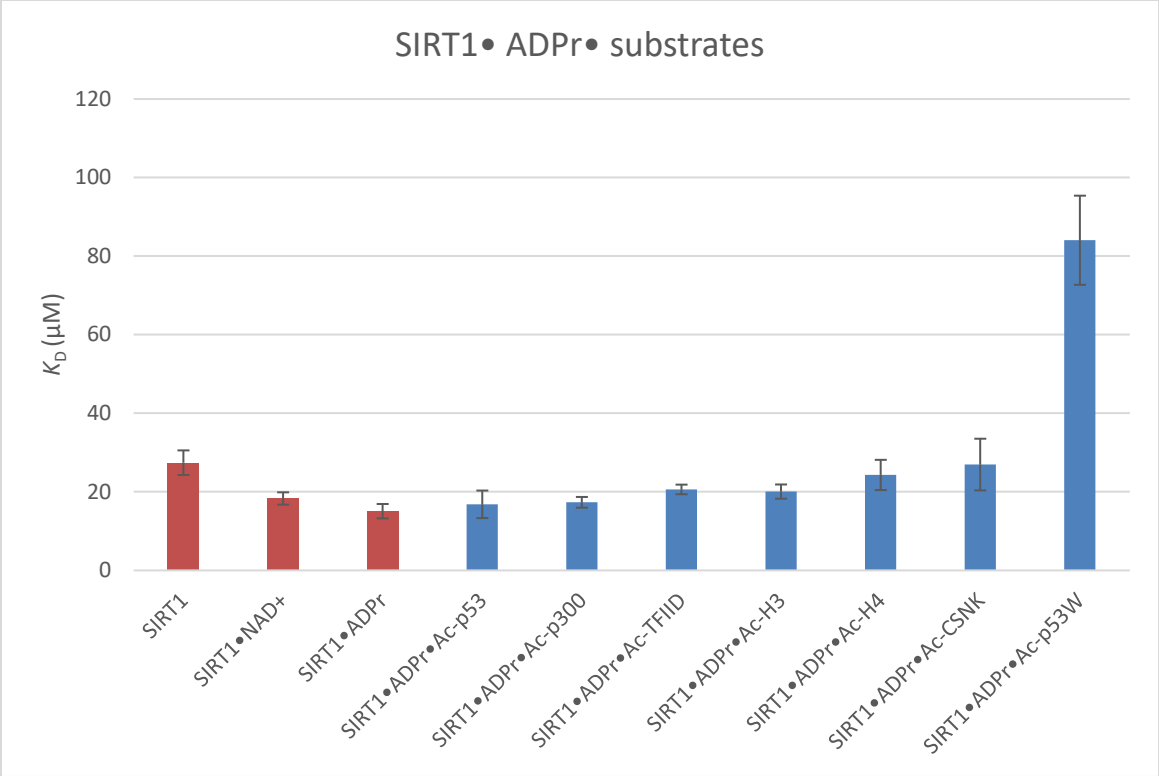

Figure 0.3. Bar graph of binding affinities between resveratrol and SIRT1 complexed with different substrates. All measurements were performed in triplicate and the average and SEM are reported. Only the binding affinity of resveratrol to the SIRT1•ADPr•Ac-p53W complex is statistically significant different (p-value < 0.05) from the binding affinity of resveratrol to apo SIRT1.According to Blaszczyk et al, the utilization of CABS-dock predictions reveals that the binding of peptide substrates to SIRT1 elicits distinctive conformational changes in both the Rossman fold domain and a specific region of the zinc binding domain located within the catalytic core.[28] These conformational shifts can be seen exclusively when the p53W peptide is bound, and are not observed in the presence of other peptide substrates. In particular, the zinc-binding domain, which is located near to the resveratrol binding sites, has two elongated -strands whereas the three -strands in the Rossman fold are moved and shortened (Figure 3.8).

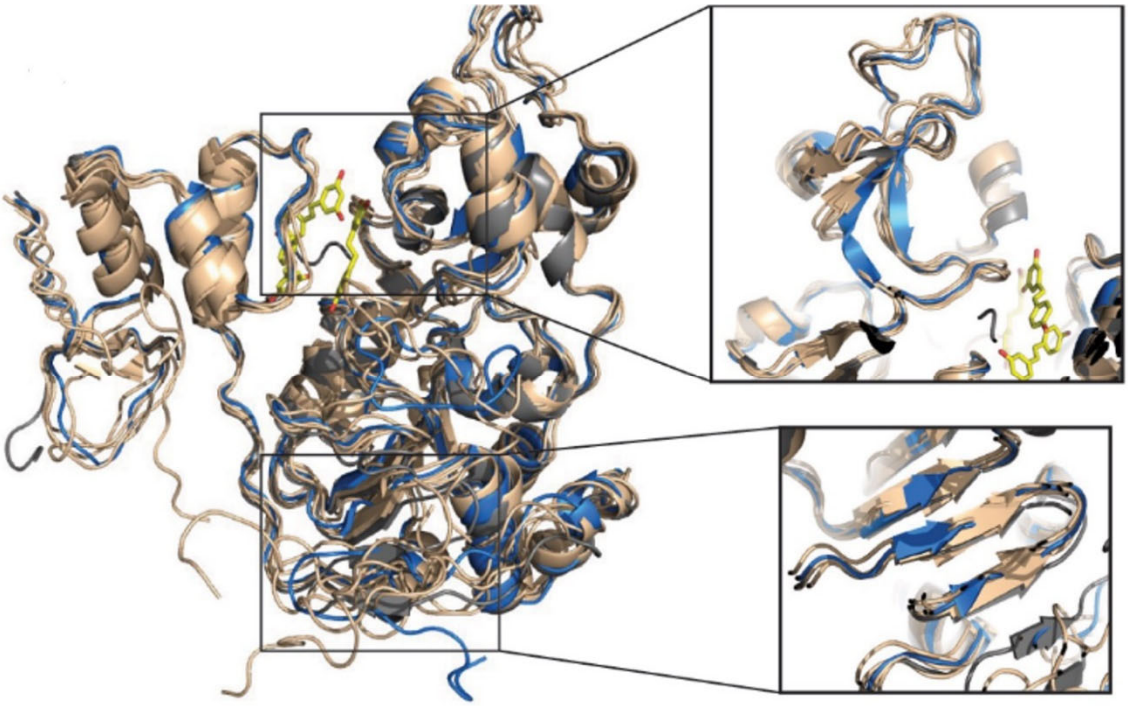

Figure 0.4. Overlay of CABS-dock structures of SIRT1-143 where the different peptide substrates were submitted as peptide ligands for docking. The original 5BTR structure is shown in gray, all the structures resulting from binding to a peptide substrate where resveratrol acts as an inhibitor are shown in tan, the structure resulting from binding to Ac-p53W, where resveratrol acts as an activator, is shown in blue. The small molecules in yellow are the 3 resveratrol molecules in 5BTR. Two regions where the blue structure shows significant deviation from all other structures are zoomed in.

4 DISCUSSION AND FUTURE DIRECTIONS

4.1. Discussion

In this thesis, we evaluated resveratrol's behavioral and structural effects on SIRT1 in the setting of a dual-acting regulator. The results indicate that resveratrol shows distinct interactions with, and exerts varying effects on, SIRT1 in activation (Ac-p53W) and inhibition (Ac-p53, Ac-H4, Ac-H3, and Ac-CSNK) situations. Kinetic studies provide strong evidence that changes in K_M values are the primary factor influencing both activation and inhibition mechanisms. These data suggest that resveratrol has an impact on the recognition of substrates by SIRT1, irrespective of the regulatory path. This conclusion is consistent with previous works that have shown the impact of resveratrol on the conformational shift of SIRT1, which subsequently affects the interaction between the substrate and the enzyme during the activation situation.[10] Additionally, the result implies that resveratrol inhibition is also likely mediated by changes in conformation. Nevertheless, our supplementary investigations on the structure and function indicate that the conformational alteration triggered by resveratrol might potentially vary between the two situations.

The DSF study revealed that resveratrol can disrupt the stability of SIRT1 in both situations. Furthermore, the SAXS profiles provided evidence that resveratrol induces changes in the structure of SIRT1, regardless of whether it is in an activated or inhibited condition. In the situation of resveratrol’s role as an activator, the conformation of SIRT1 exhibits equal extension in both the radius of gyration (R_g) and the radius of cross-sections (R_{xs}). Conversely, in the situation of inhibition, there is a more noticeable alteration in R_{xs} as opposed to R_g. It is possible to suggest that resveratrol enhances the flexibility of SIRT1

during the activation process, hence promoting increased enzymatic activity and tighter substrate binding by facilitating conformational changes upon substrate binding. Conversely, in the context of inhibition, the presence of resveratrol has the potential to induce notable modifications in the structure of proteins, leading to less affinity for substrates. Previous studies using protein nuclear magnetic resonance (NMR) have provided evidence suggesting that some regions of the substrate-binding domain (SBD) undergo a loss of structural order following interaction with the protein inhibitor PACS-2.[9] The mentioned possibilities align with our studies, which indicate that resveratrol has a comparatively less impact on the destabilization of SIRT1 in the activation situation. This is because the enhanced flexibility resulting from resveratrol's influence would lead to very little destabilization, as opposed to notable structural alterations or unfolding. Likewise, the enhanced flexibility of proteins in the context of resveratrol acting as an activator may plausibly result in an elongated protein conformation in both R_g and R_{xs}. Certainly, the outcome is both unexpected and perhaps contrary to conventional expectations. It is possible to hypothesize that the increased degree of flexibility may actually enhance the process of catalysis or substrate turnover. On the other hand, in the case of resveratrol acting as an inhibitor, conformational shifts from an ordered to a disordered state in specific regions of the protein might augment the cross-sectional area to a greater extent than the total volume (Figure 4.1).

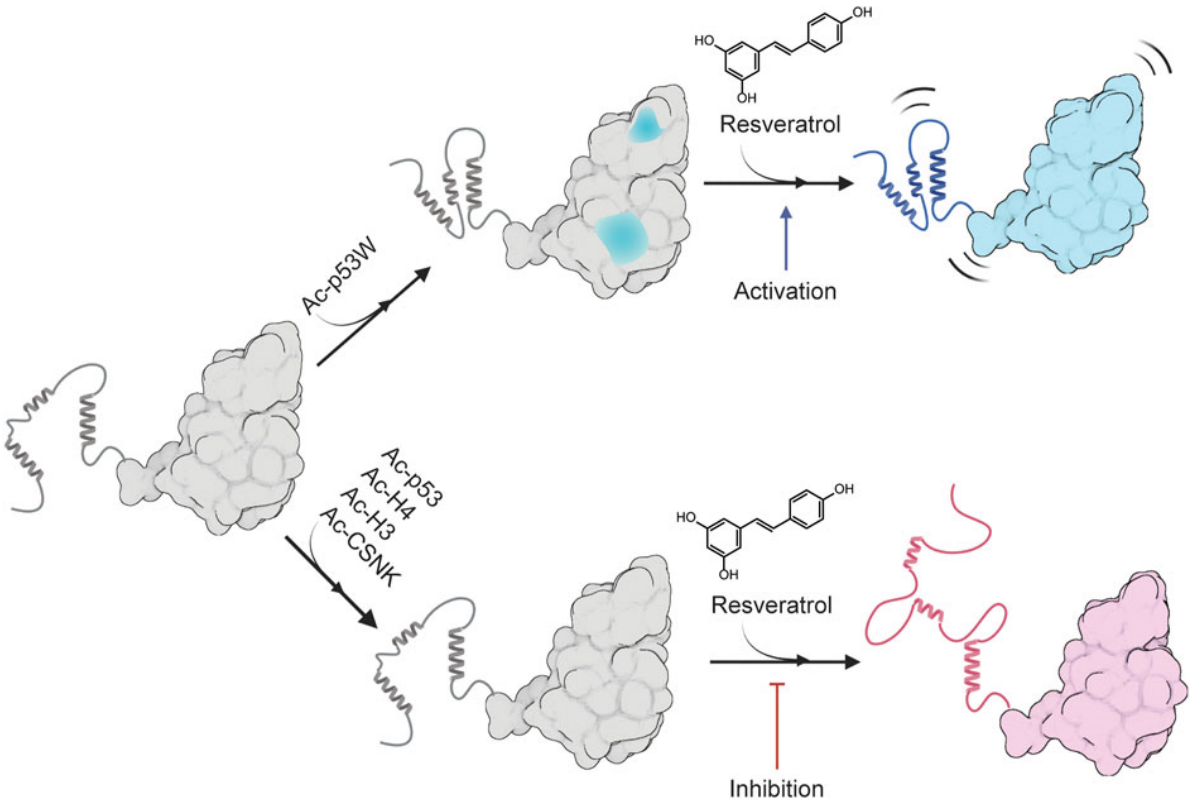

Figure 0.1. Proposed model for the peptide substrate-dependent regulation of resveratrol on SIRT1. A likely conformation of SIRT1 in solution is shown as gray, sections of SIRT1 that are predicted to undergo conformational change upon binding to Ac-p53W is shown in blue. The completely blue structure represents a more flexible SIRT1 that is activated by resveratrol, and the red structure represents a more disordered SIRT1 that is inhibited by resveratrol.

The varied effects of resveratrol on SIRT1, depending on the substrate sequence, may be attributed to its ability to activate SIRT1 via the stabilization of protein-substrate interactions.[10] This observation implies that resveratrol exhibits a selective activation of SIRT1 to substrates characterized by large K_M results. Nevertheless, the data we have obtained indicates that SIRT1 exhibits greater K_M values for all the peptide substrates in the presence of resveratrol as an inhibitor, as opposed to the activator situation. With respect to the peptide substrate sequences, it is noteworthy that in the situation where resveratrol acts as an inhibitor, the +1 position is occupied by an aliphatic residue in all substrates. In contrast,

in the case where resveratrol acts as an activator, the +1 position is occupied by an aromatic residue. Nevertheless, prior research has indicated that the activation of SIRT1 by resveratrol is not observed in certain acetyl-lysine substrates containing aromatic residues in the +1.[8] This finding suggests that the distinction between aliphatic and aromatic properties at the +1 position may not play a substantial role in the regulatory effects of resveratrol.

Interestingly, the presence of peptide substrates derived from the resveratrol-as-inhibitor experiments did not have an obvious effect on the binding affinity of resveratrol to SIRT1. However, when Ac-p53W was added to SIRT1, with resveratrol acting as an activator, there was a considerable decrease in the binding affinity of resveratrol to the enzyme. In consideration of the crystal structures reported in earlier studies, it is evident that there exist three possible locations for binding in SIRT1 for resveratrol. Based on our findings, two potential explanations might account for our observed results: (1) The interaction between Ac-p53W and SIRT1 inhibits the binding of resveratrol to its high-affinity location, or (2) it induces a conformational change in SIRT1, resulting in the binding of resveratrol to a distinct site with reduced affinity.[8] Confirming the first explanation is challenging in the absence of structural information. Therefore, techniques such as X-ray crystallography will be used in the future to obtain such information. However, analysis of CABS-dock models reveals that p53W has a distinct impact on multiple structural components of SIRT1 when interacting with various peptide substrates. Notably, p53W induces alterations in two extended β-sheets located near the resveratrol binding areas, which were initially part of a loop region. In contrast, none of the other peptides have this effect, supporting the second explanation. Furthermore, it was observed that the fluorescence emission spectrum of SIRT1 in the

presence of Ac-p53W and ADPr exhibited a distinct variation compared to the emission spectra of the other complexes. Specifically, the peak of the emission was seen at a wavelength of 359 nm, which deviated from the typical range of 330–337 nm observed in the other samples. The observed phenomenon may be ascribed to the existence of a tryptophan residue inside Ac-p53W. However, it is also plausible that a distinct alteration in the structure of SIRT1 plays a role in this disparity.

Nevertheless, these preliminary results provide a valuable contribution to our comprehension of the dual regulatory function of resveratrol on SIRT1 and have the potential to provide more insight into the underlying mechanism governing SIRT1's allosteric control. This understanding may potentially provide guidance for the development of tailored strategies to modify the activity of SIRT1 for purposes of treatment.

4.2. Future Directions

There are two main ways that the study project could go in the future. First, hydrogen-deuterium exchange can be used as a technique to enhance comprehension of the precise binding locations of distinct substrates onto SIRT1. Additionally, this will provide further insights into the extent of SIRT1's flexibility after substrate interaction and subsequent binding with resveratrol. Second, other STACs (piceatannol and SRT 1720) can be tested with SIRT1 to see if they are also substrate-specific regulators.

REFERENCES

1. Michan, S.; Sinclair, D. Sirtuins in Mammals: Insights into Their Biological Function. *Biochem. J.* **2007**, *404*, 1–13. https://doi.org/10.1042/BJ20070140.

2. Kupis, W.; Pałyga, J.; Tomal, E.; Niewiadomska, E. The Role of Sirtuins in Cellular Homeostasis. *J. Physiol. Biochem.* **2016**, *72*, 371–380. https://doi.org/10.1007/s13105-016-0492-6.

3. Rahman, S.; Islam, R. Mammalian Sirt1: Insights on Its Biological Functions. *Cell Commun. Signal.* **2011**, *9*, 11. https://doi.org/10.1186/1478-811X-9-11.

4. Davenport, A. M.; Huber, F. M.; Hoelz, A. Structural and Functional Analysis of Human SIRT1. *J. Mol. Biol.* **2014**, *426*, 526–541. https://doi.org/10.1016/j.jmb.2013.10.009.

5. Pan, M.; Yuan, H.; Brent, M.; Ding, E. C.; Marmorstein, R. SIRT1 Contains N- and C-Terminal Regions that Potentiate Deacetylase Activity. *J. Biol. Chem.* **2012**, *287*, 2468–2476. https://doi.org/10.1074/jbc.M111.285031.

6. Kang, H.; Suh, J.-Y.; Jung, Y.-S.; Jung, J.-W.; Kim, M. K.; Chung, J. H. Peptide Switch is Essential for Sirt1 Deacetylase Activity. *Mol. Cell.* **2011**, *44*, 203–213. https://doi.org/10.1016/j.molcel.2011.07.038.

7. Dai, H.; Case, A. W.; Riera, T. V.; Considine, T.; Lee, J. E.; Hamuro, Y.; Zhao, H.; Jiang, Y.; Sweitzer, S. M.; Pietrak, B.; Schwartz, B.; Blum, C. A.; Disch, J. S.; Caldwell, R.; Szczepankiewicz, B.; Oalmann, C.; Yee Ng, P.; White, B. H.; Casaubon, R.; Narayan, R.; Koppetsch, K.; Bourbonais, F.; Wu, B.; Wang, J.; Qian, D.; Jiang, F.; Mao, C.; Wang, M.; Hu, E.; Wu, J. C.; Perni, R. B.; Vlasuk, G. P.; Ellis, J. L. Crystallographic Structure of a Small Molecule SIRT1 Activator-Enzyme Complex. *Nat. Commun.* **2015**, *6*, 7645. https://doi.org/10.1038/ncomms8645.

8. Cao, D.; Wang, M.; Qiu, X.; Liu, D.; Jiang, H.; Yang, N.; Xu, R.-M. Structural Basis for Allosteric, Substrate-Dependent Stimulation of SIRT1 Activity by Resveratrol. *Genes Dev.* **2015**, *29*, 1316–1325. https://doi.org/10.1101/gad.265462.115.

9. Krzysiak, T. C.; Thomas, L.; Choi, Y.-J.; Auclair, S.; Qian, Y.; Luan, S.; Krasnow, S. M.; Thomas, L. L.; Koharudin, L. M. I.; Benos, P. V.; Marks, D. L.; Gronenborn, A. M.; Thomas, G. An Insulin-Responsive Sensor in the SIRT1 Disordered Region Binds DBC1 and PACS-2 to Control Enzyme Activity. *Mol. Cell.* **2018**, *72*, 985-998.e7. https://doi.org/10.1016/j.molcel.2018.10.007.

10. Hou, X.; Rooklin, D.; Fang, H.; Zhang, Y. Resveratrol Serves as a Protein-Substrate Interaction Stabilizer in Human SIRT1 Activation. *Sci. Rep.* **2016**, *6*, 38186. https://doi.org/10.1038/srep38186.

11. Howitz, K. T.; Bitterman, K. J.; Cohen, H. Y.; Lamming, D. W.; Lavu, S.; Wood, J. G.; Zipkin, R. E.; Chung, P.; Kisielewski, A.; Zhang, L.-L.; Scherer, B.; Sinclair, D. A. Small Molecule Activators of Sirtuins Extend Saccharomyces Cerevisiae Lifespan. *Nature.* **2003**, *425*, 191–196. https://doi.org/10.1038/nature01960.

12. Lakshminarasimhan, M.; Rauh, D.; Schutkowski, M.; Steegborn, C. Sirt1 Activation by Resveratrol is Substrate Sequence-Selective. *Aging.* **2013**, *5*, 151–154. https://doi.org/10.18632/aging.100542.

13. Zhang, M.; Lu, P.; Terada, T.; Sui, M.; Furuta, H.; Iida, K.; Katayama, Y.; Lu, Y.; Okamoto, K.; Suzuki, M.; Asakura, T.; Shimizu, K.; Hakuno, F.; Takahashi, S.-I.; Shimada, N.; Yang, J.; Ishikawa, T.; Tatsuzaki, J.; Nagata, K. Quercetin 3,5,7,3′,4′-Pentamethyl Ether from Kaempferia Parviflora Directly and Effectively Activates Human SIRT1. *Commun. Biol.* **2021**, *4*, 209. https://doi.org/10.1038/s42003-021-01705-1.

14. Pelikan, M.; Hura, G.; Hammel, M. Structure and Flexibility within Proteins as Identified through Small Angle X-Ray Scattering. *Gen. Physiol. Biophys.* **2009**, *28*, 174–189. https://doi.org/10.4149/gpb_2009_02_174.

15. Hodge, C. D.; Ismail, I. H.; Edwards, R. A.; Hura, G. L.; Xiao, A. T.; Tainer, J. A.; Hendzel, M. J.; Glover, J. N. M. RNF8 E3 Ubiquitin Ligase Stimulates Ubc13 E2 Conjugating Activity that is Essential for DNA Double Strand Break Signaling and BRCA1 Tumor Suppressor Recruitment. *J. Biol. Chem.* **2016**, *291*, 9396–9410. https://doi.org/10.1074/jbc.M116.715698.

16. Kikhney, A. G.; Svergun, D. I. A Practical Guide to Small Angle X-Ray Scattering (SAXS) of Flexible and Intrinsically Disordered Proteins. *FEBS Lett.* **2015**, *589*, 2570–2577. https://doi.org/10.1016/j.febslet.2015.08.027.

17. Smith, B. C.; Hallows, W. C.; Denu, J. M. A Continuous Microplate Assay for Sirtuins and Nicotinamide-Producing Enzymes. *Anal. Biochem.* **2009**, *394*, 101–109. https://doi.org/10.1016/j.ab.2009.07.019.

18. Chang, R. *Physical Chemistry for the Biosciences*; University Science Books: New York, 2005.

19. Classen, S.; Hura, G. L.; Holton, J. M.; Rambo, R. P.; Rodic, I.; McGuire, P. J.; Dyer, K.; Hammel, M.; Meigs, G.; Frankel, K. A.; Tainer, J. A. Implementation and Performance of SIBYLS: A Dual Endstation Small-Angle X-Ray Scattering and Macromolecular Crystallography Beamline at the Advanced Light Source. *J. Appl. Crystallogr.* **2013**, *46*, 1–13. https://doi.org/10.1107/S0021889812048698.

20. Hura, G. L.; Menon, A. L.; Hammel, M.; Rambo, R. P.; Poole II, F. L.; Tsutakawa, S. E.; Jenney, F. E. Jr.; Classen, S.; Frankel, K. A.; Hopkins, R. C.; Yang, S.; Scott, J. W.;

Dillard, B. D.; Adams, M. W. W.; Tainer, J. A. Robust, High-Throughput Solution Structural Analyses by Small Angle X-Ray Scattering (SAXS). *Nat. Methods.* **2009**, *6*, 606–612. https://doi.org/10.1038/nmeth.1353.

21. Huynh, K.; Partch, C. L. Analysis of Protein Stability and Ligand Interactions by Thermal Shift Assay. *Curr. Protoc. Protein Sci.* **2015**, *79*. https://doi.org/10.1002/0471140864.ps2809s79.

22. Shao, H.; Oltion, K.; Wu, T.; Gestwicki, J. E. Differential Scanning Fluorimetry (DSF) Screen to Identify Inhibitors of Hsp60 Protein–Protein Interactions. *Org. Biomol. Chem.* **2020**, *18*, 4157–4163. https://doi.org/10.1039/D0OB00928H.

23. Wu, T.; Yu, J.; Gale-Day, Z.; Woo, A.; Suresh, A.; Hornsby, M.; Gestwicki, J. E. Three Essential Resources to Improve Differential Scanning Fluorimetry (DSF) Experiments. *Biochem.* **2020**. https://doi.org/10.1101/2020.03.22.002543.

24. Yammine, A.; Gao, J.; Kwan, A. Tryptophan Fluorescence Quenching Assays for Measuring Protein-Ligand Binding Affinities: Principles and a Practical Guide. *BIO-Protoc.* **2019**, *9*. https://doi.org/10.21769/BioProtoc.3253.

25. Kalous, K. S.; Wynia-Smith, S. L.; Olp, M. D.; Smith, B. C. Mechanism of Sirt1 NAD+-Dependent Protein Deacetylase Inhibition by Cysteine S-Nitrosation. *J. Biol. Chem.* **2016**, *291*, 25398–25410. https://doi.org/10.1074/jbc.M116.754655.

26. Manalastas-Cantos, K.; Konarev, P. V.; Hajizadeh, N. R.; Kikhney, A. G.; Petoukhov, M. V.; Molodenskiy, D. S.; Panjkovich, A.; Mertens, H. D. T.; Gruzinov, A.; Borges, C.; Jeffries, C. M.; Svergun, D. I.; Franke, D. ATSAS 3.0: Expanded Functionality and New Tools for Small-Angle Scattering Data Analysis. *J. Appl. Crystallogr.* **2021**, *54*, 343–355. https://doi.org/10.1107/S1600576720013412.

27. Schneidman-Duhovny, D.; Hammel, M.; Tainer, J. A.; Sali, A. FoXS, FoXSDock and MultiFoXS: Single-State and Multi-State Structural Modeling of Proteins and their Complexes Based on SAXS Profiles. *Nucleic Acids Res.* **2016**, *44*, W424–W429. https://doi.org/10.1093/nar/gkw389.

28. Blaszczyk, M.; Kurcinski, M.; Kouza, M.; Wieteska, L.; Debinski, A.; Kolinski, A.; Kmiecik, S. Modeling of Protein–Peptide Interactions Using the CABS-Dock Web Server for Binding Site Search and Flexible Docking. *Methods.* **2016**, *93*, 72–83. https://doi.org/10.1016/j.ymeth.2015.07.004.